Supporting Information for
Energetics of Mammalian Cell Migration under Different Physical Conditions

Yizeng Li,[1,2,3] Lingxing Yao,[4] Yoichiro Mori,[5,6,*] and Sean X. Sun[2,3,7,†]

[1] *Department of Mechanical Engineering, Kennesaw State University, Marietta, Georgia 30060 USA*
[2] *Department of Mechanical Engineering, Johns Hopkins University, Baltimore, Maryland 21218, USA*
[3] *Institute of NanoBioTechnology, Johns Hopkins University, Baltimore, Maryland USA*
[4] *Department of Mathematics, University of Akron, Akron, Ohio 44325, USA*
[5] *Department of Mathematics and Biology, University of Pennsylvania, Philadelphia, Pennsylvania 19104, USA*
[6] *School of Mathematics, University of Minnesota, Minneapolis, Minnesota 55455, USA*
[7] *Johns Hopkins Physical Sciences-Oncology Center, Johns Hopkins University, Baltimore, Maryland 21218, USA*

CONTENTS

I. Introduction of the Two-Phase Model 1

II. One-Dimensional Model 2
A. Model Description 2
1. Governing Equations 2
2. Cell velocity v_0 as a function of j_{water} and j_{actin} 5
3. Linearization 7
B. Free Energy Identities 10
C. Minimum ATP Power Estimation 14

III. Two-Dimensional Model 16
A. Model Description 16
B. Numerical Algorithms 20
1. Fluid structure interaction substep 22
2. Semi-implicit update of IB locations 23
3. Chemical concentration substep 23
4. Time discretization at freshly cleared cell 24
5. Enforcing solute boundary condition with auxiliary variables 25
6. Network stress substep 26
C. Mechanical Energy Identities 27

References 27

I. INTRODUCTION OF THE TWO-PHASE MODEL

Cells utilize different mechanisms to migrate under different physical environments. Actin-driven cell migration is characterized by actin polymerization (depolymerization) at the cell leading (trailing) edge and the formation of focal adhesion between the actin network and the substrate.

* y1mori@sas.upenn.edu
† ssun@jhu.edu

www.pnas.org/cgi/doi/10.1073/pnas.1907625116

Water-driven cell migration is characterized by water permeation which drives membrane extension (retraction) at the cell leading (trailing) edge.

Here we describe a two-phase model with solute diffusion to unify the two distinct mechanisms of cell migration. One phase is the solvent phase, which represents the cytosol (mostly water) inside the cell and the culture medium outside of the cell. The second phase is the actin network phase which only exists inside the cell. The two phases interact with each other as well as with the physical environments. This model satisfies an energy identity and thus serves as a useful tool to study energy consumption during cell migration.

Water permeation is mainly driven by the transmembrane difference in osmotic pressure, which is determined by polarized active solute pumping on the cell membrane. In the model, when actin-driven cell migration is studied, we have chosen to mute active solute pumping. Likewise, when water-driven cell migration is studied, actin (de)polymerization is muted. The model, however, is capable of accommodating mixed modes of migration in which both mechanisms are active.

The model specifically considers the impact of the strength of focal adhesion and the coefficient of hydraulic resistance from the environments. We study the velocity of cell migration and energy consumption under these conditions.

Below, we introduce the 1D and 2D versions of the cell movement model. The simplicity of the 1D model allows for detailed theoretical investigations and extensive parameter studies, whereas the 2D model is more realistic in certain respects and allows for the exploration of fluid flow and cell shape on cell movement.

II. ONE-DIMENSIONAL MODEL

We begin with a representative 1D volume element in a moving cell. For example, for cells in 3D collagen matrices, the thin protrusions can be regarded as 1D structures (Fig. S1a). For cells on 2D substrates, a 1D strip of a cell can be modeled if velocities and forces are perpendicular to the cell leading edge. For cells in a confined space, the entire system can be modeled in 1D. Within the 1D framework, the cell boundary is reduced to a front (f) and a back (b). The schematics of the 1D model and its environment are shown in Fig. S1b.

A. Model Description

1. Governing Equations

The cell occupies a one dimensional interval on the real line, with front position given by $x = x_{\rm f}(t)$ and the back position by $x = x_{\rm b}(t)$. All functions of x to follow are thus defined for $x_{\rm b}(t) < x < x_{\rm f}(t)$. The two phases being considered is the cytosol ('c') and the actin network ('n'). Let $\theta_{\rm n}$ be the concentration of the actin network. Let θ_* be the network concentration under balance and $\theta_{\rm n}$ satisfies

$$\int_{x_{\rm b}}^{x_{\rm f}} \theta_{\rm n} dx = L\theta_*\,, \tag{II.1}$$

where $L = x_{\rm f} - x_{\rm b}$ is the length of the cell. The conservation of mass equations for the two phases are

$$\frac{\partial v_{\rm c}}{\partial x} = 0, \tag{II.2}$$

$$\frac{\partial \theta_{\rm n}}{\partial t} + \frac{\partial}{\partial x}\left(\theta_{\rm n} v_{\rm n}\right) = 0, \tag{II.3}$$

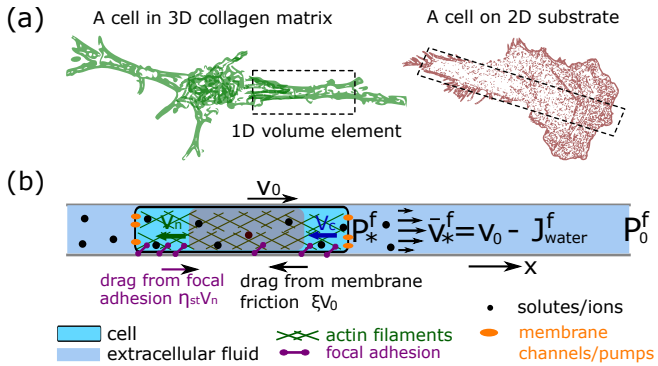

FIG. S1. Schematics of the model of cell migration. (a) Schematics of a cell in a 3D space, where the thin protrusion can be regarded as a 1D structure; a cell on a 2D substrate, where a 1D strip may be identified. (b) Diagram of a cell in a confined channel, the external fluid flow in the channel, and the relevant forces associated with cell migration. $v_{\rm n,c}$ are the F-actin network and cytosol velocities, respectively. The actin network form focal adhesion with the environment via transmembrane proteins, resulting in frictional drag force, $-\eta_{\rm st} v_{\rm n}$. Membrane movement relative to the environment also generates frictional force, $-\xi v_0$. Solutes diffuse in the cell and also being transported across the cell membrane. As the cell displaces the external water, the hydraulic pressure at the front is related to $d_g^{\rm f}(v_0 - J^{\rm f}_{\rm water})$, where v_0 is the velocity of cell migration. Quantities associated with the front of the cell are denoted by a superscript 'f'. Quantities associated with the back of the cell are not drawn.

where $v_{\rm c,n}$ are the cytosolic and network velocities. We have made the approximation that the actin network occupies no volume. Note that (II.2) implies that $v_{\rm c}$ must be constant in space, which makes it difficult in the 1D setting to study effects of fluid flow. The boundary conditions for Eq. (II.2) and (II.3) are:

$$v_{\rm c} = \dot{x}_{\rm f}(t) + j^{\rm f}_{\rm water}\,, \ \text{at } x = x_{\rm f}(t), \tag{II.4}$$
$$v_{\rm c} = \dot{x}_{\rm b}(t) - j^{\rm b}_{\rm water}\,, \ \text{at } x = x_{\rm b}(t), \tag{II.5}$$
$$\theta_{\rm n} v_{\rm n} = \theta_{\rm n}\dot{x}_{\rm f}(t) + j^{\rm f}_{\rm actin}\,, \ \text{at } x = x_{\rm f}(t), \tag{II.6}$$
$$\theta_{\rm n} v_{\rm n} = \theta_{\rm c}\dot{x}_{\rm b}(t) - j^{\rm b}_{\rm actin}\,, \ \text{at } x = x_{\rm b}(t). \tag{II.7}$$

In the above, $\dot{x}_{\rm f,b}$ denotes the time derivative and $j^{\rm f,b}_{\rm water}$ is the water flux at the front and back and $j^{\rm f,b}_{\rm actin}$ is the actin polymerization rate at the front and back respectively. Both $j^{\rm f,b}_{\rm water}$ and $j^{\rm f,b}_{\rm actin}$ are defined positive outward. We assume that we are at steady state, so that the cell is moving at a constant speed $\dot{x}_{\rm f} = \dot{x}_{\rm b} = v_0$, and that the state of the cell is stationary with respect to the coordinate system moving at speed v_0. From this, we see that equations (II.2) and (II.3) can be written as:

$$\frac{\partial}{\partial x}(v_{\rm c} - v_0) = 0, \tag{II.8}$$
$$\frac{\partial}{\partial x}(\theta_{\rm n}(v_{\rm n} - v_0)) = 0, \tag{II.9}$$

and the boundary conditions above can be written as:

$$(v_{\rm c} - v_0)|_{x_{\rm f}} = j^{\rm f}_{\rm water} = -j_{\rm water} = -j^{\rm b}_{\rm water} = (v_{\rm c} - v_0)|_{x_{\rm b}}\,, \tag{II.10}$$
$$\theta_{\rm n}(v_{\rm n} - v_0)|_{x_{\rm f}} = j^{\rm f}_{\rm actin} = -j_{\rm actin} = -j^{\rm b}_{\rm actin} = \theta_{\rm n}(v_{\rm n} - v_0)|_{x_{\rm b}}\,. \tag{II.11}$$

We now turn to force balance. This is written as:

$$-\frac{\partial p}{\partial x} - \eta\theta_{\rm n}(v_{\rm c} - v_{\rm n}) = 0, \tag{II.12}$$

$$-\frac{\partial \sigma}{\partial x} + \eta\theta_{\rm n}(v_{\rm c} - v_{\rm n}) - \eta_{\rm st}\theta_{\rm n} v_{\rm n} = 0. \tag{II.13}$$

where σ is the pressure generated by the cytoskeletal network. η is the coefficient of the interface drag between the actin network and the cytosol. $\eta_{\rm st}$ is the coefficient of the focal adhesion depending on the stiffness of substrate [1, 2] and the size [3] and density [4] of adhesions. We have neglected the shear viscous term within each phase because these are much smaller than the interface drag. The two fluids may also experience drags from the nucleus when cells are confined in narrow channels. These drags can be incorporated into the model if needed.

The network pressure has a passive component, $\sigma_{\rm n}(\theta_{\rm n})$, coming from the constitutive relation of the network and an active component, $\sigma_{\rm a}$, coming from the myosin contraction within the network, i.e.,

$$\sigma = \sigma_{\rm n}(\theta_{\rm n}) + \sigma_{\rm a}. \tag{II.14}$$

In all simulation results in this paper, $\sigma_{\rm a}$ is set to 0. We shall nonetheless retain this term in the theoretical calculations as it leads to some additional insight. We use an uni-axial swelling model [5] for the passive stress,

$$\sigma_{\rm n} = -RT\rho_{\rm n}\left(\frac{\theta_0}{\theta_{\rm n}} - \frac{\theta_{\rm n}}{2\theta_0}\right), \tag{II.15}$$

where R is the ideal gas constant, T is the absolute temperature, $\rho_{\rm n}$ is the actin molar density, and $\theta_0 = \theta_*/\sqrt{2}$ is a constant such that $\sigma_{\rm n} = 0$ when $\theta_{\rm n} = \theta_*$.

The boundary conditions for the above force balance equations are given by:

$$b[p_*^{\rm f} - (\sigma + p)] = -2\tau^{\rm f} + bf_{\rm ext}^{\rm f}, \text{ at } x = x_{\rm f}(t), \tag{II.16}$$

$$b[p_*^{\rm b} - (\sigma + p)] = -2\tau^{\rm b} + bf_{\rm ext}^{\rm b}, \text{ at } x = x_{\rm b}(t), \tag{II.17}$$

where b is the width of the cell strip, $p_*^{\rm f,b}$ are the pressures of the fluid just outside of the cell at $x^{\rm f,b}$, $\tau^{\rm f,b}$ are tensions of the membrane at $x^{\rm f,b}$, and $f_{\rm ext}^{\rm f,b}$ are the externally applied forces at the front and back defined positive in the positive norm direction of the cell boundary. The expressions for $p_*^{\rm f,b}$ are

$$p_*^{\rm f} = p_\infty^{\rm f} + d_g^{\rm f}(v_0 - j_{\rm water}),\ p_*^{\rm b} = p_\infty^{\rm b} - d_g^{\rm b}(v_0 - j_{\rm water}), \tag{II.18}$$

where $p_\infty^{\rm f,b}$ are the pressures of the fluid at $x = \pm\infty$ respectively and $d_g^{\rm f,b}$ is the coefficient of hydraulic resistance due to the outside fluid flow. We note that this term linear in $v_0 - j_{\rm water}$ is an approximation at best; indeed, in a 1D model, the outside fluid has no flow field structure. A proper treatment of hydraulic resistance, therefore, requires a 2D model, which we discuss later. Finally, we have the following equation for force balance of the membrane (which we have assumed is moving at velocity v_0):

$$2(\tau^{\rm f} - \tau^{\rm b}) = 2\xi L v_0. \tag{II.19}$$

We next consider the solute diffusion part which is linked to the osmolarity of the system. For simplicity, we consider only one solute species. We have:

$$\frac{\partial c}{\partial t} + \frac{\partial}{\partial x}(v_{\rm c} c) = \frac{\partial}{\partial x}\left(D\frac{\partial c}{\partial x}\right), \tag{II.20}$$

where c is the molar concentration of the solute and D is the diffusion constant. Given our assumption on stationarity, we have:

$$\frac{\partial}{\partial x}((v_{\rm c}-v_0)c)=\frac{\partial}{\partial x}\left(D\frac{\partial c}{\partial x}\right). \tag{II.21}$$

As for boundary conditions, we have:

$$\left((v_{\rm c}-v_0)c-D\frac{\partial c}{\partial x}\right)\Big|_{x_{\rm f}}=j_{\rm sol}^{\rm f}\,, \tag{II.22}$$

$$\left((v_{\rm c}-v_0)c-D\frac{\partial c}{\partial x}\right)\Big|_{x_{\rm b}}=-j_{\rm sol}^{\rm b}\,, \tag{II.23}$$

where $j_{\rm sol}^{\rm f,b}$ is the transmembrane solute flux and we have assumed that fluxes are positive outward. By (II.21), we must have:

$$-j_{\rm sol}^{\rm f}=j_{\rm sol}^{\rm b}\equiv j_{\rm sol}. \tag{II.24}$$

We may specify $j_{\rm sol}^{\rm f,b}$ as follows:

$$j_{\rm sol}^{\rm f}=k_{\rm sol}^{\rm f}\triangle c^{\rm f}+i_{\rm sol}^{\rm f},\ j_{\rm sol}^{\rm b}=k_{\rm sol}^{\rm b}\triangle c^{\rm b}+i_{\rm sol}^{\rm b}\,,\ \triangle c^{\rm f,b}=c^{\rm f,b}-c_{\infty}^{\rm f,b}\,, \tag{II.25}$$

where $j_{\rm sol}$ is written as a sum of the passive solute flux, proportional to the difference in concentrations across the membrane and $i_{\rm sol}$ which is the actively generated pump flux. The concentration $c^{\rm f,b}$ denotes the (intracellular) concentration c at $x=x_{\rm f,b}$ and $c_{\infty}^{\rm f,b}$ is the extracellular concentration just outside $x=x_{\rm f,b}$. We have here assumed that the solute concentration is spatially uniform in the extracellular space. The expression of water flux is given by

$$j_{\rm water}^{\rm f}=\alpha_{\rm f}\triangle\psi^{\rm f},\ j_{\rm water}^{\rm b}=\alpha_{\rm b}\triangle\psi^{\rm b},\ \triangle\psi^{\rm f,b}=\triangle p^{\rm f,b}-RT\triangle c^{\rm f,b},\ \triangle p^{\rm f,b}=p|_{x_{\rm f,b}}-p_{*}^{\rm f,b} \tag{II.26}$$

where RT is the product of the ideal gas constant and the absolute temperature and $p|_{x_{\rm f,b}}$ denote the intracellular pressures at the front and back of the cell respectively. The quantity $\triangle\psi^{\rm f,b}$ is the difference in water potential across the membrane.

The primary variables to the system are p, $v_{\rm c}$, $v_{\rm n}$, $\theta_{\rm n}$, c, and v_0. The equations used to solve these variables are Eqs. (II.8), (II.9), (II.12), (II.13), (II.21), and (II.29). The boundary conditions for Eqs. (II.8), (II.9), (II.12), (II.13) are Eqs. (II.1), (II.4), (II.6), and (II.10); the boundary conditions for Eq. (II.21) are Eqs. (II.22) and (II.23). The above will give us a full solution to the problem. In a later section (Sec. II A 3) we will discuss a linearized solution.

The basic parameters for the model are listed in Tab. S1. Unless otherwise specified, these parameters are used throughout the paper.

2. Cell velocity v_0 as a function of $j_{\rm water}$ and $j_{\rm actin}$

We next derive the dependence of v_0 on $j_{\rm actin}$ and $j_{\rm water}$. Adding (II.12), (II.13) and integrating the sum from $x_{\rm b}$ to $x_{\rm f}$, we have,

$$(-\sigma-p)|_{x_{\rm b}}^{x_{\rm f}}-\int_{x_{\rm b}}^{x_{\rm f}}\eta_{\rm st}\theta_{\rm n}v_{\rm n}dx=0. \tag{II.27}$$

Combining this with (II.19), we have:

$$2(\tau^{\rm f}-\tau^{\rm b})+b\,(-\sigma-p)|_{x_{\rm b}}^{x_{\rm f}}-b\int_{x_{\rm b}}^{x_{\rm f}}\eta_{\rm st}\theta_{\rm n}v_{\rm n}dx-2\xi Lv_0=0\,, \tag{II.28}$$

TABLE S1. Parameters used in the 1D model. These are the default parameters unless otherwise specified.

Parameters	Description	Values	Sources
R (J/mol K)	Ideal gas constant	8.31451	Constant
T (K)	Absolute temperature	300	Room temperature
k_B (J/K)	Boltzmann constant	1.38×10^{-23}	Constant
N_A (1/mol)	Avogadios number	6.02×10^{23}	Constant
L (μm)	Cell length	50	Generic
b (μm)	Cell width	3	Generic
w (μm)	Cell height	10	Generic
h (μm)	membrane thickness	0.5	Ref. [6]
η (Pa·s/μm^2)	Drag coefficient between two phases	1	Ref. [7]
ξ (Pa·s/μm)	Coefficient of friction of the channel wall	1	Based on Ref. [8]
$\eta_{\rm st}$ (Pa·s/μm^2)	Coefficient of drag from focal adhesion	1×10^4	Based on Ref. [9]
d_g (Pa·s/μm)	Coefficient of hydraulic pressure	1×10^3	Ref. [8]
D (μm^2/s)	Diffusion coefficient of solute	1	Ref. [8]
$k_{\rm sol}^{\rm f}$ (μm/s)	Passive channel coefficient at the front	50	Assumed
$k_{\rm sol}^{\rm b}$ (μm/s)	Passive channel coefficient at the back	50	Assumed
$i_{\rm sol}^{\rm f}$ (mol/m^2·s)	Active solute flux at the front	6.25×10^{-7}	Assumed
$i_{\rm sol}^{\rm b}$ (mol/m^2·s)	Active solute flux at the back	6.25×10^{-7}	Assumed
$f_{\rm ext}^{\rm f}$ (Pa)	External force per unit area at the front	0	Generic
$f_{\rm ext}^{\rm b}$ (Pa)	External force per unit area at the back	0	Generic
$\alpha^{\rm f}$ (μm/(Pa·s))	Water permeability constant at the front	1.0×10^{-4}	Ref. [8]
$\alpha^{\rm b}$ (μm/(Pa·s))	Water permeability constant at the back	1.0×10^{-4}	Ref. [8]
θ_*	Average concentration of the actin phase	0.02	Based on Ref. [10]
ρ_n (mM)	Molar density of the actin network	3.4	Based on Ref. [11]
$j_{\rm actin}$ (nm/s)	Actin flux at the two boundaries	$10\theta_*$	Assumed
$p_\infty^{\rm f}$ (Pa)	extracellular hydrostatic pressure at the front	0	Generic
$p_\infty^{\rm b}$ (Pa)	extracellular hydrostatic pressure at the back	0	Generic
$c_\infty^{\rm f}$ (mM)	extracellular ion concentration at the front	340	Ref. [8]
$c_\infty^{\rm b}$ (mM)	extracellular ion concentration at the back	340	Ref. [8]
$A_{\rm F}$ (nm^2)	Cross sectional area of one actin filament	25	Based on Ref. [12]
δ (nm)	Effective length of each G-actin	3	Based on Ref. [13]
$G_{\rm ATP}$ (J)	Energy consumption of each ATP	$25k_BT \approx 100$ pN·nm	Ref. [14]
n_a	Number of ATPs each G-actin assembling takes	1	Scaled
n_c	Number of ATPs each pumped ion takes	1	Scaled

where ξ is the coefficient of membrane friction with the surroundings. Using (II.16) and (II.17), we thus have

$$b\,(f_{\rm ext} - p_*)|_{x_{\rm b}}^{x_{\rm f}} = b\int_{x_{\rm b}}^{x_{\rm f}} \eta_{\rm st}\theta_{\rm n} v_{\rm n} dx + 2\xi L v_0\,. \tag{II.29}$$

In the case of $f_{\rm ext} = 0$ and $p_\infty^{\rm f} = p_\infty^{\rm b}$, we then have,

$$-\,b d_g(v_0 - j_{\rm water}) = b\int_{x_{\rm b}}^{x_{\rm f}} \eta_{\rm st}\theta_{\rm n} v_{\rm n} dx + 2\xi L v_0\,, \tag{II.30}$$

where $d_g = d_g^{\rm f} + d_g^{\rm b}$ is the effective, total coefficient of external hydraulic resistance. According to (II.11), we get

$$v_0 = \frac{\eta_{\rm st}}{\theta_*\eta_{\rm st} + 2\widehat{\xi} + \widehat{d}_g} j_{\rm actin} + \frac{\widehat{d}_{\rm g}}{\theta_*\eta_{\rm st} + 2\widehat{\xi} + \widehat{d}_g} j_{\rm water},\ \widehat{\xi} = \frac{\xi}{b},\ \widehat{d}_g = \frac{d_g}{L}. \tag{II.31}$$

This is an exact expression as no approximation is introduced during the derivation. If water flux is known a priori, the cell velocity can be estimated accordingly, but the solutions to other variables remain unknown.

Equation (II.31) shows that cell migration can be actin-driven (the fist term) or water-driven (the second term). The cell velocity v_0 is a linear function of $j_{\rm actin}$ and $j_{\rm water}$, with each coefficient being a nonlinear function in both $\eta_{\rm st}$ and d_g. The $j_{\rm actin}$ term dominates when $\eta_{\rm st}$ is large; and the $j_{\rm water}$ term dominates when d_g is large. The actin-driven velocity attains its maximum at $v_0 = j_{\rm actin}/\theta_*$ and the water-driven velocity attains its maximum at $v_0 = j_{\rm water}$.

3. Linearization

Let us now solve the full equations in Sec. II A 1 for small velocity. We shall henceforth assume that the external force $f_{\rm ext}$ is equal to 0, active stress $\sigma_{\rm a} = 0$ and in (II.18) and (II.25), we set

$$p_\infty^{\rm f} = p_\infty^{\rm b}\,,\quad d_g^{\rm f} = d_g^{\rm b} = \frac{d_g}{2}\,,\quad c_\infty^{\rm f} = c_\infty^{\rm b}\,. \tag{II.32}$$

We first consider the resting state when $i_{\rm sol}$ and $j_{\rm actin}$ are equal to 0. In this case, we should have:

$$v_{\rm n} = v_{\rm c} = v_0 = 0. \tag{II.33}$$

From (II.12), p is constant in space, whose value we shall call $p_{\rm r}$. From (II.13), we then have that σ must be equal to a constant. Let us assume that σ is an increasing function of $\theta_{\rm n}$. This will then imply that $\theta_{\rm n}$ is also constant, which we denote by $\theta_{\rm n,r}$. $\theta_{\rm n,r} = \theta_*$ by definition.

Let us now linearize, assuming the input, $j_{\rm water}$ and $j_{\rm actin}$ are small. Equations (II.10) and (II.11) yield:

$$(v_{\rm c} - v_0) = -j_{\rm water},\ \theta_{\rm n,r}(v_{\rm n} - v_0) = -j_{\rm actin}\,. \tag{II.34}$$

The term $j_{\rm water}$ is given as in (II.26). Consider the case when

$$\alpha_{\rm f} = \alpha_{\rm b} = \alpha. \tag{II.35}$$

In addition, in equation (II.25) we let:

$$k_{\rm sol}^{\rm f,b} = k_{\rm sol},\ -i_{\rm sol}^{\rm f} = i_{\rm sol} = i_{\rm sol}^{\rm b}. \tag{II.36}$$

Note first that, when $i_{\rm sol} = 0$, by (II.26) and (II.25), we must have:

$$p_{\rm r} = p_\infty^{\rm f,b}\,,\quad c = c_{\rm r} = c_\infty^{\rm f,b}. \tag{II.37}$$

We now seek to express v_0 in terms of $i_{\rm sol}$ and $j_{\rm actin}$. To do so, first note that (II.12), to leading order, gives:

$$-\frac{\partial p}{\partial x} - \eta\theta_{\rm n,r}(v_{\rm c} - v_{\rm n}) = 0. \tag{II.38}$$

Substituting (II.34) into the above, we have:

$$\frac{\partial p}{\partial x} = \widetilde{\eta} j_{\text{water}} - \eta j_{\text{actin}} \equiv A_p,\ \widetilde{\eta} = \eta \theta_{\text{n,r}}. \tag{II.39}$$

From this, we see that:

$$p(x) = B_p + A_p \left(x - \frac{x_{\text{f}} + x_{\text{b}}}{2} \right). \tag{II.40}$$

To determine B_p, we may argue as follows. Using (II.35), we find that:

$$-\triangle p^{\text{f}} = \triangle p^{\text{b}}. \tag{II.41}$$

With (II.37), we find:

$$p^{\text{f}} - (p_{\text{r}} + d_g^{\text{f}}(v_0 - j_{\text{water}}) = -\left(p^{\text{b}} - (p_{\text{r}} - d_g^{\text{b}}(v_0 - j_{\text{water}})) \right). \tag{II.42}$$

We have:

$$\frac{1}{2}(p^{\text{f}} + p^{\text{b}}) = p_{\text{r}}. \tag{II.43}$$

Thus, $B_p = p_{\text{r}}$ and

$$p^{\text{f}} = p_{\text{r}} + \frac{A_p L}{2},\ p^{\text{b}} = p_{\text{r}} - \frac{A_p L}{2}. \tag{II.44}$$

Using (II.22) and (II.23), we have:

$$\frac{\partial c}{\partial x} = \frac{1}{D}(-j_{\text{water}} c + j_{\text{sol}}) \equiv A_c. \tag{II.45}$$

Using (II.25), we have:

$$A_c = \frac{1}{D}\left(-j_{\text{water}} c_{\text{r}} - \frac{k_{\text{sol}} L}{2} A_{\text{c}} + i_{\text{sol}} \right). \tag{II.46}$$

Thus,

$$A_c = \frac{1}{D + k_{\text{sol}} L/2}(-j_{\text{water}} c_{\text{r}} + i_{\text{sol}}). \tag{II.47}$$

Combining this with (II.39), we have:

$$A_p - RT A_c = (\widetilde{\eta} + \zeta c_{\text{r}}) j_{\text{water}} - \eta j_{\text{actin}} - \zeta i_{\text{sol}},\ \zeta = \frac{RT}{D + k_{\text{sol}} L/2}, \tag{II.48}$$

From (II.26), we have:

$$j_{\text{water}} = -\alpha \left(\frac{(A_p - RT A_c) L}{2} - \frac{d_g}{2}(v_0 - j_{\text{water}}) \right). \tag{II.49}$$

Using (II.48), we have:

$$\left(2 + \widehat{\alpha}\left(d_g + (\widetilde{\eta} + \zeta c_{\text{r}})\right)\right) j_{\text{water}} = \widehat{\alpha}\left(\widehat{d_g} v_0 + \eta j_{\text{actin}} + \zeta i_{\text{sol}} \right),\quad \widehat{\alpha} = \alpha L\,. \tag{II.50}$$

We may now plug this into (II.31) to obtain the cell velocity under linearization,

$$v_{0,L} = \frac{1}{K_c}\left(\left(\eta_{\rm st} + \frac{\eta\widehat{\alpha}\widehat{d}_g}{2+\widehat{\alpha}(\widehat{d}_g+\widetilde{\eta}+\zeta c_{\rm r})}\right) j_{\rm actin} + \frac{\zeta\widehat{\alpha}\widehat{d}_g}{2+\widehat{\alpha}(\widehat{d}_g+\widetilde{\eta}+\zeta c_{\rm r})} i_{\rm sol}\right),$$
$$K_c = \frac{\left(\theta_*\eta_{\rm st} + 2\widehat{\xi} + \widehat{d}_g\right)\left(2+\widehat{\alpha}(\widehat{d}_g+\widetilde{\eta}+\zeta c_{\rm r})\right) - \widehat{\alpha}\widehat{d}_g{}^2}{2+\widehat{\alpha}(\widehat{d}_g+\widetilde{\eta}+\zeta c_{\rm r})}. \tag{II.51}$$

A comparison of the predicted cell velocity from the numerical simulations of the model in Sec. II A 1 and Eq. (II.51) is shown in Fig. S2. We can see that the results are almost identical, demonstrating that the regime over which the linear approximation is valid is quite broad.

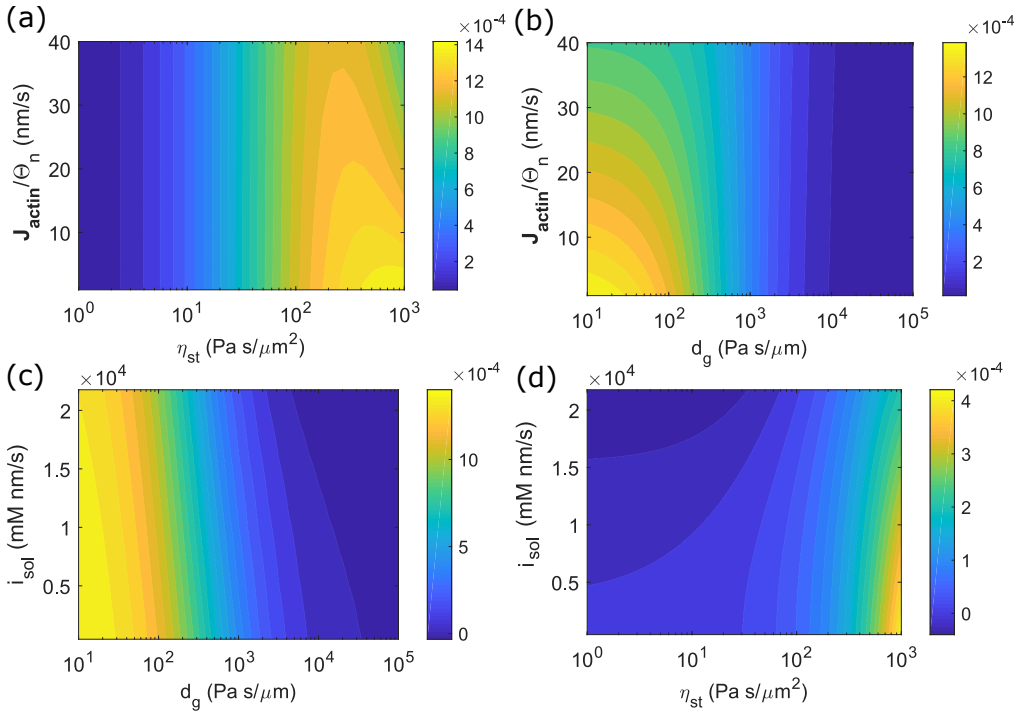

FIG. S2. Comparison of the predicted cell velocity from the full model and the model of linearization. The contours of $(v_0 - v_{0,L})/v_0$ are plotted to indicate the relative difference between the two computational schemes. (a) $d_g = 0$ and $i_{\rm sol}^{\rm f} = -i_{\rm sol}^{\rm b} = 0$. (b) $\eta_{\rm st} = 10^3$ Pa·s/μm^2 and $i_{\rm sol}^{\rm f} = -i_{\rm sol}^{\rm b} = 0$. (c) $j_{\rm actin} = 0$, $i_{\rm sol}^{\rm f} = -i_{\rm sol}^{\rm b} = i_{\rm sol}$, and $\eta_{\rm st} = 10^3$ Pa·s/μm^2. (d) $j_{\rm actin} = 0$, $i_{\rm sol}^{\rm f} = -i_{\rm sol}^{\rm b} = i_{\rm sol}$, and $d_g = 10^2$ Pa·s/μm.

Equation (II.51) shows that an increase in α generally leads to an increase in the speed. The parameters associated with water flux and hydraulic resistance, i.e., α and d_g, enter into the $j_{\rm actin}$ term, suggesting that when $\alpha d_g \neq 0$, the flow dynamics affects the contribution of actin polymerization on cell migration. In particular, in an environment where focal adhesion is not available and cells do not generate active solute pumping, i.e., $\eta_{\rm st} = 0$ and $i_{\rm sol} = 0$, cells may still be able to migrate through actin polymerization alone, i.e.,

$$v_{0,L} = \left[\frac{\eta\theta_*\widehat{\alpha}\widehat{d}_g}{2\widehat{\xi}\left(2+\widehat{\alpha}(\widehat{d}_g+\eta\theta_*+\zeta c_{\rm r})\right) + \widehat{d}_g\left(2+\widehat{\alpha}\left(\eta\theta_*+\zeta c_r\right)\right)}\right]\frac{j_{\rm actin}}{\theta_*}. \tag{II.52}$$

We can see that the coefficient of $j_{\rm actin}/\theta_*$ in the brackets is always less than 1, meaning that without focal adhesion, cells cannot attain the maximum velocity set by the rate of actin polymerization

(compare to Eq. II.31). This coefficient increases with increasing η, $\widehat{\alpha}$, $\widehat{d_g}$, or $k_{\rm sol}$. For example, figure S3 shows the contour of the coefficient as η and α vary. We can see that at extreme high η, which is the drag coefficient between the actin network and the cytosol, the cells can reach more than 20% of the velocity from $j_{\rm actin}/\theta_*$. Although such a high η may not be realistic since we do not expect the friction between actin and cytosol being similar to that from focal adhesion, we would like to point out that water permeation induced by actin polymerization is also a possible mechanism of cell migration.

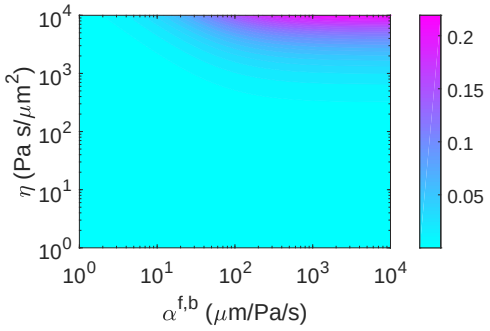

FIG. S3. The contour of the coefficient of $j_{\rm actin}/\theta_*$ in Eq. II.52 (the expression within the brackets) as η and α vary. Here $\eta_{\rm st} = 0$ and $i_{\rm sol} = 0$, other parameters are listed in Tab. S1.

B. Free Energy Identities

Recall that the passive actin network pressure, σ, has two components, $\sigma = \sigma_{\rm n}(\theta_{\rm n}) + \sigma_{\rm a}$, where $\sigma_{\rm n}$ is given by Eq. (II.15). We first define the energy density $e_{\rm n}$ associated with the passive actin network pressure $\sigma_{\rm n}$. as satisfying the following differential equation:

$$\theta_{\rm n}\frac{de_{\rm n}}{d\theta_{\rm n}} - e_{\rm n} = \theta_{\rm n}^2\frac{d}{d\theta_{\rm n}}\left(\frac{e_{\rm n}}{\theta_{\rm n}}\right) = \sigma_{\rm n}(\theta_{\rm n}). \tag{II.53}$$

The energy density $e_{\rm n}$ can be solved from Eq. (II.53) with Eq. (II.15). It is easily checked that $e_{\rm n}$ must be a convex function of $\theta_{\rm n}$. The constant of integration is determined by

$$\left.\frac{de_{\rm n}}{d\theta_{\rm n}}\right|_{\theta_{\rm n}=\theta_*} = 0\,, \tag{II.54}$$

such that the convex function $e_{\rm n}$ reaches its minimum at $\theta_{\rm n} = \theta_*$. With Eq. (II.53) we have:

$$\frac{\partial\sigma_{\rm n}}{\partial x} = \theta_{\rm n}\frac{\partial}{\partial x}\left(\frac{de_{\rm n}}{d\theta_{\rm n}}\right)\,, \tag{II.55}$$

which will be used in the energy identities derived below.

We now compute the energy relation satisfied by the model. Multiply (II.12) by $v_{\rm c}$ and (II.13) by $v_{\rm n}$ and integrate from $x_{\rm b}$ to $x_{\rm f}$, and add the two resulting expressions. We have:

$$\int_{x_{\rm b}}^{x_{\rm f}}\left(-v_{\rm c}\frac{\partial p}{\partial x} - v_{\rm n}\frac{\partial\sigma_{\rm n}}{\partial x}\right)dx - \int_{x_{\rm b}}^{x_{\rm f}}\left(\eta\theta_{\rm n}(v_{\rm c}-v_{\rm n})^2 + \eta_{\rm st}\theta_{\rm n}v_{\rm n}^2\right)dx = 0 \tag{II.56}$$

Consider the first integral. We have:

$$\begin{aligned}
&\int_{x_\mathrm{b}}^{x_\mathrm{f}} \left(-v_\mathrm{c} \frac{\partial p}{\partial x} - v_\mathrm{n} \left(\theta_\mathrm{n} \frac{\partial}{\partial x} \left(\frac{de_\mathrm{n}}{d\theta_\mathrm{n}} \right) + \frac{\partial \sigma_\mathrm{a}}{\partial x} \right) \right) dx \\
&= \left(-pv_\mathrm{c} - \left(\theta_\mathrm{n} \frac{de_\mathrm{n}}{d\theta_\mathrm{n}} + \sigma_\mathrm{a} \right) v_\mathrm{n} \right) \Big|_{x_\mathrm{b}}^{x_\mathrm{f}} + \int_{x_\mathrm{b}}^{x_\mathrm{f}} \left(p \frac{\partial v_\mathrm{c}}{\partial x} + \frac{de_\mathrm{n}}{d\theta_\mathrm{n}} \frac{\partial (\theta_\mathrm{n} v_\mathrm{n})}{\partial x} + \sigma_\mathrm{a} \frac{\partial v_\mathrm{n}}{\partial x} \right) dx \\
&= \left(-pv_\mathrm{c} - \left(\theta_\mathrm{n} \frac{de_\mathrm{n}}{d\theta_\mathrm{n}} + \sigma_\mathrm{a} \right) v_\mathrm{n} + e_\mathrm{n} v_0 \right) \Big|_{x_\mathrm{b}}^{x_\mathrm{f}} + \int_{x_\mathrm{b}}^{x_\mathrm{f}} \sigma_\mathrm{a} \frac{\partial v_\mathrm{n}}{\partial x} dx,
\end{aligned} \tag{II.57}$$

where we integrated by parts in the first equality and used (II.8) and (II.9) in the second equality. Let us consider the boundary term in the last line above. The boundary term at x_f may be evaluated as follows:

$$\begin{aligned}
&- pv_\mathrm{c} - \left(\theta_\mathrm{n} \frac{de_\mathrm{n}}{d\theta_\mathrm{n}} + \sigma_\mathrm{a} \right) v_\mathrm{n} + e_\mathrm{n} v_0 = -pv_0 - pj^\mathrm{f}_\mathrm{water} - \left(\theta_\mathrm{n} \frac{de_\mathrm{n}}{d\theta_\mathrm{n}} + \sigma_\mathrm{a} \right) \frac{j^\mathrm{f}_\mathrm{actin}}{\theta_\mathrm{n}} - \sigma v_0 \\
&= \left(-\frac{2\tau^\mathrm{f}}{b} - p^\mathrm{f}_* + f^\mathrm{f}_\mathrm{ext} \right) v_0 - pj^\mathrm{f}_\mathrm{water} - \left(\frac{de_\mathrm{n}}{d\theta_\mathrm{n}} - \frac{\sigma_\mathrm{a}}{\theta_\mathrm{n}} \right) j^\mathrm{f}_\mathrm{actin} \\
&= \left(-\frac{2\tau^\mathrm{f}}{b} + f^\mathrm{f}_\mathrm{ext} \right) v_0 - p^\mathrm{f}_* (v_0 + j^\mathrm{f}_\mathrm{water}) - (p - p^\mathrm{f}_*) j^\mathrm{f}_\mathrm{water} - \left(\frac{de_\mathrm{n}}{d\theta_\mathrm{n}} + \frac{\sigma_\mathrm{a}}{\theta_\mathrm{n}} \right) j^\mathrm{f}_\mathrm{actin}.
\end{aligned} \tag{II.58}$$

In the above, we used (II.10) and (II.11) in the first equality and (II.16) in the second equality. We have retained the superscript $^\mathrm{f}$ in j_water and j_actin for later convenience. At x_b, we obtain, in the same way, the following expression:

$$\begin{aligned}
&- pv_\mathrm{c} - \left(\theta_\mathrm{n} \frac{de_\mathrm{n}}{d\theta_\mathrm{n}} + \sigma_\mathrm{a} \right) v_\mathrm{n} + e_\mathrm{n} v_0 \\
&= \left(-\frac{2\tau^\mathrm{b}}{b} + f^\mathrm{b}_\mathrm{ext} \right) v_0 - p^\mathrm{b}_* (v_0 - j^\mathrm{b}_\mathrm{water}) + (p - p^\mathrm{b}_*) j^\mathrm{b}_\mathrm{water} + \left(\frac{de_\mathrm{n}}{d\theta_\mathrm{n}} + \frac{\sigma_\mathrm{a}}{\theta_\mathrm{n}} \right) j^\mathrm{b}_\mathrm{actin}.
\end{aligned} \tag{II.59}$$

Combining the above expressions, we have:

$$\begin{aligned}
&\left(-pv_\mathrm{c} - \left(\theta_\mathrm{n} \frac{de_\mathrm{n}}{d\theta_\mathrm{n}} + \sigma_\mathrm{a} \right) v_\mathrm{n} + e_\mathrm{n} v_0 \right) \Big|_{x_\mathrm{b}}^{x_\mathrm{f}} = \left(-\frac{2(\tau^\mathrm{f} - \tau^\mathrm{b})}{b} + f^\mathrm{f}_\mathrm{ext} - f^\mathrm{b}_\mathrm{ext} \right) v_0 \\
&- (p^\mathrm{f}_* - p^\mathrm{b}_*)(v_0 - j_\mathrm{water}) - \triangle p^\mathrm{f} j^\mathrm{f}_\mathrm{water} - \triangle p^\mathrm{b} j^\mathrm{b}_\mathrm{water} + \left(\frac{de_\mathrm{n}}{d\theta_\mathrm{n}} + \frac{\sigma_\mathrm{a}}{\theta_\mathrm{n}} \right) \Big|_{x_\mathrm{b}}^{x_\mathrm{f}} j_\mathrm{actin}.
\end{aligned} \tag{II.60}$$

Equations (II.19), (II.56), (II.57) and (II.60) together yields:

$$\begin{aligned}
&b \left(\left(f^\mathrm{f}_\mathrm{ext} - f^\mathrm{b}_\mathrm{ext} \right) v_0 - (p^\mathrm{f}_* - p^\mathrm{b}_*)(v_0 - j_\mathrm{water}) \right) \\
&+ b \left(-\triangle p^\mathrm{f} j^\mathrm{f}_\mathrm{water} - \triangle p^\mathrm{b} j^\mathrm{b}_\mathrm{water} + \left(\frac{de_\mathrm{n}}{d\theta_\mathrm{n}} + \frac{\sigma_\mathrm{a}}{\theta_\mathrm{n}} \right) \Big|_{x_\mathrm{b}}^{x_\mathrm{f}} j_\mathrm{actin} + \int_{x_\mathrm{b}}^{x_\mathrm{f}} \sigma_\mathrm{a} \frac{\partial v_\mathrm{n}}{\partial x} dx \right) \\
&= b \int_{x_\mathrm{b}}^{x_\mathrm{f}} \left(\eta \theta_\mathrm{n} (v_\mathrm{c} - v_\mathrm{n})^2 + \eta_\mathrm{st} \theta_\mathrm{n} v_\mathrm{n}^2 \right) dx + 2\xi L v_0^2.
\end{aligned} \tag{II.61}$$

Multiply (II.21) by $\ln c$ and integrate from x_b to x_f:

$$\begin{aligned}
&\int_{x_\mathrm{b}}^{x_\mathrm{f}} \ln c \frac{\partial}{\partial x} \left(-(v_\mathrm{c} - v_0) c + D \frac{\partial c}{\partial x} \right) dx \\
&= - \left(j^\mathrm{f}_\mathrm{sol} \ln c^\mathrm{f} + j^\mathrm{b}_\mathrm{sol} \ln c^\mathrm{b} \right) + \int_{x_\mathrm{b}}^{x_\mathrm{f}} \left((v_\mathrm{c} - v_0) \frac{\partial c}{\partial x} - Dc \left(\frac{\partial}{\partial x} \ln c \right)^2 \right) dx \\
&= - \left(j^\mathrm{f}_\mathrm{sol} \ln c^\mathrm{f} + j^\mathrm{b}_\mathrm{sol} \ln c^\mathrm{b} \right) - j_\mathrm{water} (c^\mathrm{f} - c^\mathrm{b}) - \int_{x_\mathrm{b}}^{x_\mathrm{f}} Dc \left(\frac{\partial}{\partial x} \ln c \right)^2 dx = 0,
\end{aligned} \tag{II.62}$$

where we used (II.22) and (II.23) in the first equality and (II.10) in the second equality. Multiply the above by bRT and add to (II.61):

$$\begin{aligned}
&b\left(\left(f^{\mathrm{f}}_{\mathrm{ext}}-f^{\mathrm{b}}_{\mathrm{ext}}\right)v_0-(p^{\mathrm{f}}_*-p^{\mathrm{b}}_*)(v_0-j_{\mathrm{water}})-RT\triangle c_\infty j_{\mathrm{water}}-RT\left(j^{\mathrm{f}}_{\mathrm{sol}}\ln c^{\mathrm{f}}+j^{\mathrm{b}}_{\mathrm{sol}}\ln c^{\mathrm{b}}\right)\right)\\
&+b\left(-\triangle\psi^{\mathrm{f}}j^{\mathrm{f}}_{\mathrm{water}}-\triangle\psi^{\mathrm{b}}j^{\mathrm{b}}_{\mathrm{water}}+\left(\frac{de_{\mathrm{n}}}{d\theta_{\mathrm{n}}}+\frac{\sigma_{\mathrm{a}}}{\theta_{\mathrm{n}}}\right)\Big|_{x_{\mathrm{b}}}^{x_{\mathrm{f}}}j_{\mathrm{actin}}+\int_{x_{\mathrm{b}}}^{x_{\mathrm{f}}}\sigma_{\mathrm{a}}\frac{\partial v_{\mathrm{n}}}{\partial x}dx\right)\\
=&b\int_{x_{\mathrm{b}}}^{x_{\mathrm{f}}}\left(\eta\theta_{\mathrm{n}}(v_{\mathrm{c}}-v_{\mathrm{n}})^2+\eta_{\mathrm{st}}\theta_{\mathrm{n}}v_{\mathrm{n}}^2\right)dx+2\xi Lv_0^2+bRT\int_{x_{\mathrm{b}}}^{x_{\mathrm{f}}}Dc\left(\frac{\partial}{\partial x}\ln c\right)^2dx,
\end{aligned}\tag{II.63}$$

where $\triangle c_\infty=c^{\mathrm{f}}_\infty-c^{\mathrm{b}}_\infty$. Note that:

$$j^{\mathrm{f}}_{\mathrm{sol}}\ln c^{\mathrm{f}}=j^{\mathrm{f}}_{\mathrm{sol}}\ln c^{\mathrm{f}}_\infty+j_{\mathrm{sol}}\ln\left(\frac{c^{\mathrm{f}}}{c^{\mathrm{f}}_\infty}\right)=j^{\mathrm{f}}_{\mathrm{sol}}\ln c^{\mathrm{f}}_\infty+\left(k^{\mathrm{f}}_{\mathrm{sol}}\triangle c^{\mathrm{f}}+i^{\mathrm{f}}_{\mathrm{sol}}\right)\ln\left(\frac{c^{\mathrm{f}}}{c^{\mathrm{f}}_\infty}\right).\tag{II.64}$$

Working likewise on at x_{b} and combining this with the above, we have:

$$\begin{aligned}
j^{\mathrm{f}}_{\mathrm{sol}}\ln c^{\mathrm{f}}+j^{\mathrm{b}}_{\mathrm{sol}}\ln c^{\mathrm{b}}=&-j_{\mathrm{sol}}\ln\left(\frac{c^{\mathrm{f}}_\infty}{c^{\mathrm{b}}_\infty}\right)+i^{\mathrm{f}}_{\mathrm{sol}}\ln\left(\frac{c^{\mathrm{f}}}{c^{\mathrm{f}}_\infty}\right)+i^{\mathrm{b}}_{\mathrm{sol}}\ln\left(\frac{c^{\mathrm{b}}}{c^{\mathrm{b}}_\infty}\right)\\
&+k^{\mathrm{f}}_{\mathrm{sol}}\triangle c^{\mathrm{f}}\ln\left(\frac{c^{\mathrm{f}}}{c^{\mathrm{f}}_\infty}\right)+k^{\mathrm{b}}_{\mathrm{sol}}\triangle c^{\mathrm{b}}\ln\left(\frac{c^{\mathrm{b}}}{c^{\mathrm{b}}_\infty}\right)
\end{aligned}\tag{II.65}$$

where we used (II.24). Using (II.65) and (II.26) in (II.63), we obtain:

$$\mathcal{I}_{\mathrm{ext}}+\mathcal{I}_{\mathrm{cell}}=\mathcal{D}_{\mathrm{fric}}+\mathcal{D}_{\mathrm{flow}}+\mathcal{D}_{\mathrm{sol}},\tag{II.66}$$

$$\mathcal{I}_{\mathrm{ext}}=bw\left(\left(f^{\mathrm{f}}_{\mathrm{ext}}-f^{\mathrm{b}}_{\mathrm{ext}}\right)v_0-\triangle p_\infty v_0+\triangle\psi_\infty j_{\mathrm{water}}+\triangle\mu_\infty j_{\mathrm{sol}}\right),\tag{II.67}$$

$$\mathcal{I}_{\mathrm{cell}}=bw\left(-\triangle\mu^{\mathrm{f}}i^{\mathrm{f}}_{\mathrm{sol}}-\triangle\mu^{\mathrm{b}}i^{\mathrm{b}}_{\mathrm{sol}}+\left(\frac{de_{\mathrm{n}}}{d\theta_{\mathrm{n}}}+\frac{\sigma_{\mathrm{a}}}{\theta_{\mathrm{n}}}\right)\Big|_{x_{\mathrm{b}}}^{x_{\mathrm{f}}}j_{\mathrm{actin}}+\int_{x_{\mathrm{b}}}^{x_{\mathrm{f}}}\sigma_{\mathrm{a}}\frac{\partial v_{\mathrm{n}}}{\partial x}dx\right),\tag{II.68}$$

$$\mathcal{D}_{\mathrm{fric}}=bw\int_{x_{\mathrm{b}}}^{x_{\mathrm{f}}}\left(\eta\theta_{\mathrm{n}}(v_{\mathrm{c}}-v_{\mathrm{n}})^2+\eta_{\mathrm{st}}\theta_{\mathrm{n}}v_{\mathrm{n}}^2\right)dx+2\xi Lwv_0^2,\tag{II.69}$$

$$\mathcal{D}_{\mathrm{flow}}=bw\left(\alpha_{\mathrm{f}}(\triangle\psi^{\mathrm{f}})^2+\alpha_{\mathrm{b}}(\triangle\psi^{\mathrm{b}})^2+d_g(v_0-j_{\mathrm{water}})^2\right),\tag{II.70}$$

$$\mathcal{D}_{\mathrm{sol}}=bw\left(k^{\mathrm{f}}_{\mathrm{sol}}\triangle c^{\mathrm{f}}\triangle\mu^{\mathrm{f}}+k^{\mathrm{b}}_{\mathrm{sol}}\triangle c^{\mathrm{b}}\triangle\mu^{\mathrm{b}}+RT\int_{x_{\mathrm{b}}}^{x_{\mathrm{f}}}Dc\left(\frac{\partial}{\partial x}\ln c\right)^2dx\right),\tag{II.71}$$

where w is the height of the cell and

$$\begin{aligned}
&\triangle\psi_\infty=\triangle p_\infty-RT\triangle c_\infty,\\
&\triangle\mu_\infty=RT\ln\left(\frac{c^{\mathrm{f}}_\infty}{c^{\mathrm{b}}_\infty}\right),\ \triangle\mu^{\mathrm{f,b}}=RT\ln\left(\frac{c^{\mathrm{f,b}}}{c^{\mathrm{f,b}}_\infty}\right).
\end{aligned}\tag{II.72}$$

The above is the energy relation for the model. The term $\mathcal{I}_{\mathrm{ext}}$ is energy input due to external environmental or experimental manipulation. The term $\mathcal{I}_{\mathrm{cell}}$ is the energy input from mechanisms that the cell controls, including the solute pumps, actin polymerization, and cytoskeletal force generation. Since we are at steady state, all energy input is dissipated. This dissipation is given as three terms $\mathcal{D}_{\mathrm{fric}}$, $\mathcal{D}_{\mathrm{flow}}$, and $\mathcal{D}_{\mathrm{sol}}$. All of the three dissipation terms are positive ($\triangle c^{\mathrm{f,b}}$ and $\triangle\mu^{\mathrm{f,b}}$ always have the same sign). The dissipation $\mathcal{D}_{\mathrm{fric}}$ comes from the various friction forces; $\mathcal{D}_{\mathrm{flow}}$ comes from the passive transmembrane water flux and dissipation in the exterior fluid; $\mathcal{D}_{\mathrm{sol}}$ is the solute diffusive dissipation inside the cell and at the membrane.

We may check that the above energy relation does not change upon adding an arbitrary constant to the pressure p, since, in all places where the pressure appears, it appears in the form of differences. It is to be emphasized that an arbitrarily written model does not satisfy an energy identity of the above type, in which the dissipation is demonstrably positive. For example, our prescription of (II.18) is the only possible linear relation for $p_* - p_\infty$ if we want the external fluid to have a dissipative effect.

The mechanical power dissipation derived in Eqs. (II.69)–(II.71) can be individually analyzed. For example, under actin-driven cell migration, where there is no water flow across the cell membrane, we can calculate the power dissipation through the interface (the first term in Eq. II.69), the focal adhesion (the second term in Eq. II.69), and the membrane friction (the third term in Eq. II.69).

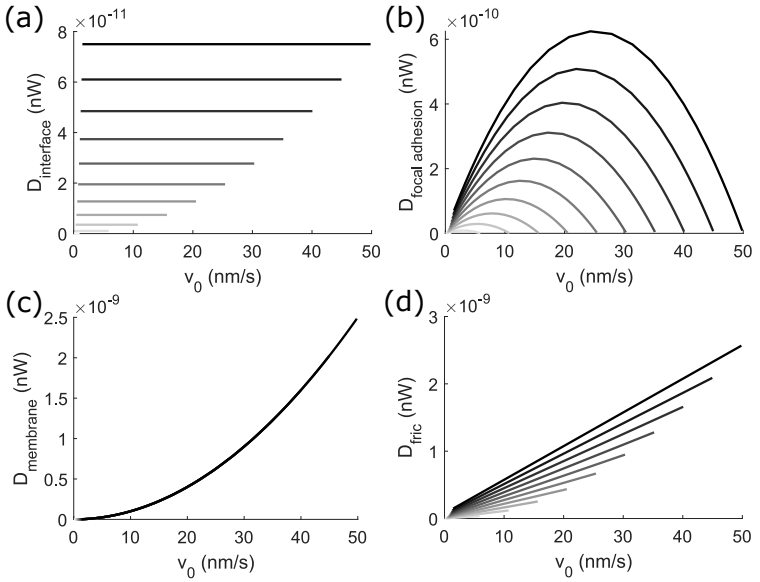

FIG. S4. Power dissipation of actin-driven cell migration through various frictional terms, including (a) the power dissipation through the interface (the first term in Eq. II.69), (b) the focal adhesion (the second term in Eq. II.69), (c) the membrane friction (the third term in Eq. II.69, and (d) the total friction as a sum of the above three (Eq. II.69). Each term is plotted as a function of v_0 for different rates of actin polymerization. The velocity field is extracted from Fig. 1c. Different lines represent different $j_{\rm actin}/\theta_*$ ranging linearly from 1 nm/s to 5 nm/s, as indicted in Fig. 1c. Darker lines represent higher rates of actin polymerization. Within each line, $\eta_{\rm st}$ increases from left to right. In (c), all the lines overlap. The lines for lower values of $j_{\rm actin}/\theta_*$ are shorter and closer to the original point.

We next examine the contribution of each power term in Eq. II.66 to the total power consumption. In actin-driven cell migration (represented by Fig. 1c) without water flux, the power is almost solely dissipated through the friction, $\mathcal{D}_{\rm fric}$, and the amount of dissipation increases with v_0 through increasing $\eta_{\rm st}$ (Fig. S5a, where the lines for the total dissipation and $\mathcal{D}_{\rm fric}$ overlap). In water-driven cell migration (represented by Fig. 1e) without actin polymerization, 80–90% of the total power is dissipated through the solute/ion diffusion at the membrane and within the cell, $\mathcal{D}_{\rm sol}$ (Fig. S5b). The passive water flux through the cell membrane and the dissipation through the external fluid, $\mathcal{D}_{\rm flow}$, contributes 10–20% of the total power dissipation and the dissipation through the friction, $\mathcal{D}_{\rm fric}$, is negligible (Fig. S5b). The total power generation and dissipation increase with increasing $i^{\rm f}_{\rm sol}$ but are almost constant in v_0, which is determined by d_g in this case.

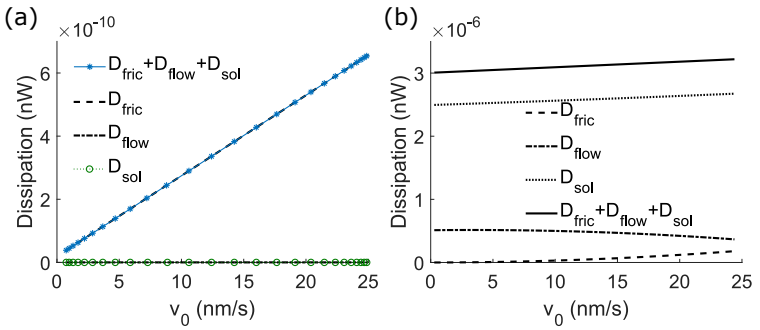

FIG. S5. Mechanical Power Dissipation. (a) Power dissipation of actin-driven cell migration as v_0 increases with $\eta_{\rm st}$. $j_{\rm actin}/\theta_* = 25.5$ nm/s and $i_{\rm sol} = 0$. The velocities are extracted from Fig. 1(c). (b) Power dissipation of water-driven cell migration as v_0 increases with d_g. $i^{\rm f}_{\rm sol} = 3.16\times10^{-5}$ mol/m^2·s and $j_{\rm actin} = 0$.

C. Minimum ATP Power Estimation

The driving mechanism for cell migration are actin polymerization and water flux; the latter mainly comes from active solute pumping across the cell. The minimum ATP power consumption associated with actin polymerization and solute pumping can be calculated. Denote $G_{\rm ATP}$ as the hydrolysis energy for one ATP.

In actin polymerization, the effective velocity of actin polymerization at the cell front is $j_{\rm actin}/\theta^{\rm f}_{\rm n}$, where $\theta^{\rm f}_{\rm n}$ is the volume occupation of the actin network at the front of the cell. The number of ATP needed to sustain such velocity per second per F-actin filament is $n_a j_{\rm actin}/\theta^{\rm f}_{\rm n}\delta$, where δ is the length of a G-actin monomer and n_a is the number of ATP needed to complete one G-actin-to-F-actin assembling. The number of F-actin filament at the cell front can be estimated from its concentration. Denote $A = bw$ as the cross-sectional area of a 1D cell and A_F as the cross-sectional area of one F-actin filament. We then have $N_F = A\theta^{\rm f}_{\rm n}/A_F$ number of F-actin filament at the polymerizing front of the cell. We can write out the ATP power associated with actin polymerization as

$$\mathcal{P}_{\rm actin} = N_F \frac{j_{\rm actin}}{\theta^{\rm f}_{\rm n}\delta} G_{\rm ATP} n_a \,, \tag{II.73}$$

which is a linear function in $j_{\rm actin}$ (Fig. S6a).

In active solute pumping, the flux, $i_{\rm sol}$, is in the unit of molar per meter squared per second. To convert solute flux into the number of solutes, we will need the cross-sectional area of the cell and the Avogadro's number N_A. The ATP power associated with active solute pumping is

$$\mathcal{P}_{\rm sol} = AN_A n_c G_{\rm ATP}(|i^{\rm b}_{\rm sol}| + |i^{\rm f}_{\rm sol}|) \,, \tag{II.74}$$

which is a linear function in $|i^{\rm b}_{\rm sol}| + |i^{\rm f}_{\rm sol}|$ (Fig. S6b). n_c is the average number of ATP needed to pump one solute across the cell membrane. Living cells continuously use ATPs to pump solutes. When cells are not polarized and $i^{\rm b}_{\rm sol} = i^{\rm f}_{\rm sol}$, $\mathcal{P}_{\rm sol}$ can be very large but there is no water flux comes directly from solute pumping. Hence, $\mathcal{P}_{\rm sol}$ does not always imply cell migration. To investigate the ATP power of solute pumping that directly results in cell migration, we only consider the minimum $\mathcal{P}_{\rm sol}$ needed to generate solute concentration that leads to water flux. As a convention, in this work $\mathcal{P}_{\rm sol} = 0$ means no minimum asymmetric active pumping that generates water flux.

We next analyze the ATP power consumption of cell migration by using the linearized cell

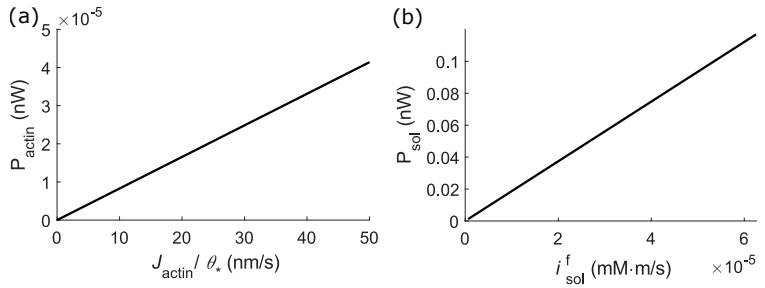

FIG. S6. ATP power consumption for actin polymerization (a) is about four order of magnitudes smaller than the power consumption of active solute pump (b). Scaled by $n_a = 1$ and $n_c = 1$. In (b), we vary $i^{\rm f}_{\rm sol}$ from 6.25×10^{-7} mM·m/s to 6.25×10^{-5} mM·m/s and keep $i^{\rm b}_{\rm sol} = 0$.

velocity. Substituting (II.73) and (II.74) into (II.51) gives

$$v_{0,L} = \left(\frac{\eta_{\rm st} + \eta\lambda}{K_c}\right) \frac{A_F\delta}{AG_{\rm ATP}n_a}\mathcal{P}_{\rm actin} + \left(\frac{\zeta c_r\lambda}{K_c}\right) \frac{1}{2N_A c_r AG_{\rm ATP}n_c}\mathcal{P}_{\rm sol}\,, \tag{II.75}$$
$$\lambda = \frac{\widehat{\alpha}\widehat{d}_g}{2 + \widehat{\alpha}(\widehat{d}_g + \eta\theta_* + \zeta c_r)}\,,$$

which tells us how much $\mathcal{P}_{\rm actin}$ or $\mathcal{P}_{\rm sol}$ is needed to achieve some v_0 because the coefficients before $\mathcal{P}_{\rm actin}$ and $\mathcal{P}_{\rm sol}$ determine the corresponding power needed to generate v_0. Based on the parameters in Tab. S1, we can estimate the orders of magnitude as follows.

In Eq. (II.75), both $A_F\delta$ and $N_A c_r$ are close to the order of 10 nm^3 so the factors outside the brackets are of the same dimension and order of magnitude for the two terms. Therefore, only the coefficients in the brackets in (II.75) determines the relative contribution of $\mathcal{P}_{\rm actin}$ and $\mathcal{P}_{\rm sol}$ to the cell velocity. For values in Tab. S1, $D \ll k_{\rm sol}L$ so that $\zeta \approx 2RT/k_{\rm sol}L$ by (II.48) is on the order of 1 J·s/μm^2·mol. ζc_r is thus on the order of 100 Pa·s/μm^2, which is much larger than $\eta\theta_*$. In this case, (II.75) can be reduced to

$$v_{0,L} = \frac{1}{K_c}\left[\eta_{\rm st} + \underbrace{\frac{\eta\widehat{\alpha}\widehat{d}_g}{2 + \widehat{\alpha}(\widehat{d}_g + \zeta c_r)}}_{\rm term1}\right] \frac{A_F\delta}{AG_{\rm ATP}n_a}\mathcal{P}_{\rm actin} + \frac{1}{K_c}\left[\underbrace{\frac{\zeta c_r\widehat{\alpha}\widehat{d}_g}{2 + \widehat{\alpha}(\widehat{d}_g + \zeta c_r)}}_{\rm term2}\right] \frac{1}{2N_A c_r AG_{\rm ATP}n_c}\mathcal{P}_{\rm sol}\,, \tag{II.76}$$

where K_c is also reduced to

$$K_c = \frac{\left(\theta_*\eta_{\rm st} + 2\widehat{\xi} + \widehat{d}_g\right)\left(2 + \widehat{\alpha}(\widehat{d}_g + \zeta c_{\rm r})\right) - \widehat{\alpha}\widehat{d}_g{}^2}{2 + \widehat{\alpha}(\widehat{d}_g + \zeta c_{\rm r})} = \left(\theta_*\eta_{\rm st} + 2\widehat{\xi}\right) + \frac{2\widehat{d}_g\left(1 + \widehat{\alpha}\zeta c_{\rm r}\right)}{2 + \widehat{\alpha}(\widehat{d}_g + \zeta c_{\rm r})}\,. \tag{II.77}$$

When $d_g < 1$ Pa·s/μm, $\eta_{\rm st}$, which varies from 1 to 10^4 Pa·s/μm^2, is up to four orders larger than $\zeta c_r\lambda$ (see Fig. S7a). In this case, a much smaller $\mathcal{P}_{\rm actin}$ than $\mathcal{P}_{\rm sol}$ is needed to generate a non-trivial v_0. When d_g increases, $\zeta c_r\lambda$ may become comparable to $\eta_{\rm st}$, depending on the $\eta_{\rm st}$. On the other hand, the denominator K_c increases almost linearly with d_g up to $d_g \sim 10^6$ Pa·s/μm (see Fig. S7b), which means the attainable v_0 reduces with increasing d_g so that moderate $\mathcal{P}_{\rm actin}$ can no longer generate the same v_0. When d_g is large, a commensurate increase in $\mathcal{P}_{\rm sol}$ is necessary to compensate for the reduced attainable v_0. For parameter values used above, the maximum values of the term 2 does not exceed the maximum value of $\eta_{\rm st}$ (see Fig. S7a), the ATP power consumption from active

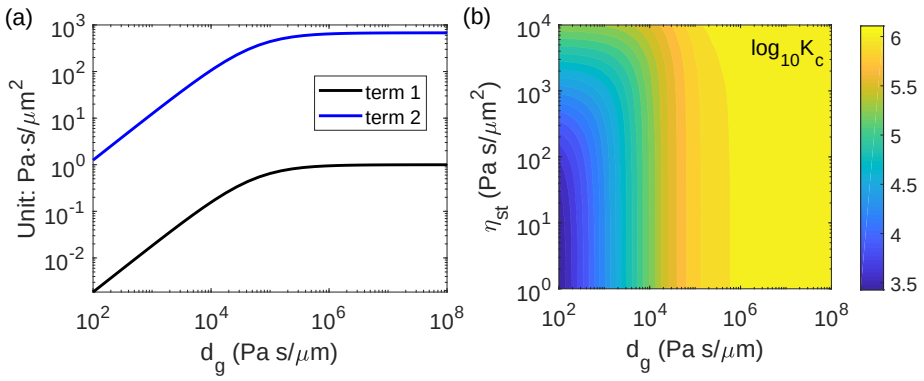

FIG. S7. Variation of some coefficients. (a) The variations of term 1 and term 2 in Eq. II.76 as functions of d_g. (b) Contour of $\log_{10}K_c$ as $\eta_{\rm st}$ and d_g vary. K_c is in the unit of Pa·s/μm^2.

solute pumping is always higher than that of actin polymerization. We do note, however, that this ratio is highly dependent on the choice of $k_{\rm sol}$, which could be different, or indeed controlled by the cell. A lower $k_{\rm sol}$ can make the water-driven mechanism more efficient.

The picture that emerges is as follows. From Eq. (II.75) we can see that $\eta_{\rm st}$ is the effective force coefficient acting on the actin network and $\zeta c_r \lambda$ is the effective force coefficient acting on the solute. The effectiveness of the two mechanisms depend largely on the relative magnitude of these two numbers. For low hydraulic resistance, the effective drag on the solute is lower than that on the actin network, making actin polymerization more effective for cell migration. For high hydraulic resistance, the effective drag $\zeta c_{\rm r}\lambda$ on the solute increases, making water driven cell migration more effective. The overall attainable velocity decreases, however, because of the increasing frictional factor represented by K_c.

III. TWO-DIMENSIONAL MODEL

The basic physical picture behind the 2D model is the same as the 1D model, although the formulations of the equations are somewhat more involved. The model and numerical method presented here is a direct outgrowth of [15]. The novelty in relation to [15] is the addition of actin network dynamics.

A. Model Description

We consider a 2D computational domain Ω that is separated into intracellular and extracellular regions $\Omega_{\rm i}$ and $\Omega_{\rm e}$ by the cell membrane Γ (Fig. S8a, a top view of the cell sitting on a 2D substrate). The cell membrane position is given by $\boldsymbol{x} = \boldsymbol{X}(s,t)$, where $s \in \mathbb{R}/(2\pi\mathbb{Z})$ is the material coordinate and t is time. We denote the intracellular side of the membrane Γ as $\Gamma_{\rm i}$ and the extracellular side as $\Gamma_{\rm e}$. On Γ the unit normal is $\boldsymbol{n}$, pointing outward from the $\Gamma_{\rm i}$ side to the $\Gamma_{\rm e}$ side. The unknown functions are the membrane position $\boldsymbol{X}$, the fluid velocity $\boldsymbol{v}_{\rm c}$, pressure p and solute concentration c defined in Ω, and the actin network velocity, $\boldsymbol{v}_{\rm n}$, and concentration, $\theta_{\rm n}$, both defined inside the intracellular space $\Omega_{\rm i}$.

On the inlet and outlet of the computational domain, periodic boundary conditions are enforced for $\boldsymbol{v}_{\rm c}$, p, and c. On the channel walls of the computational domain, non-slip boundary condition is enforced for $\boldsymbol{v}_{\rm c}$; zero-gradient boundary condition is enforced for p, and non-flux boundary condition is enforced for c.

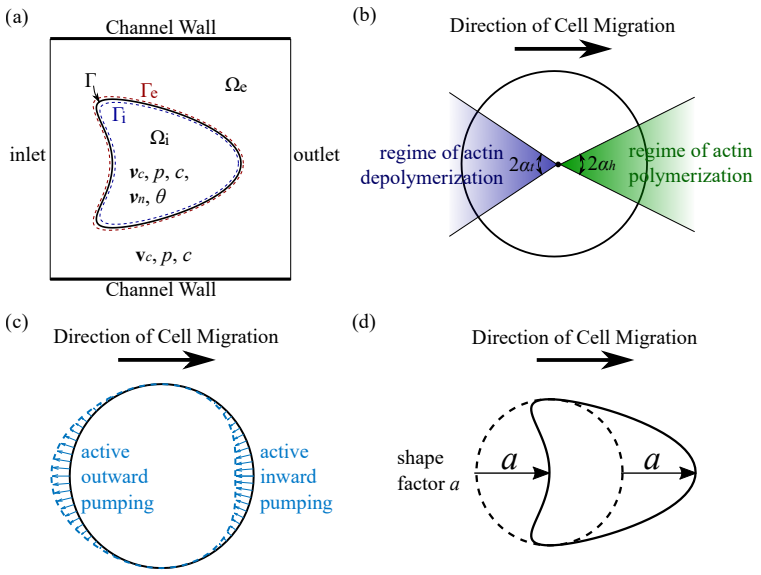

FIG. S8. (a) Schematics of the 2D computational domain from a top view. Γ represents the cell membrane that separates the intracellular domain $\Omega_{\rm i}$ and the extracellular domain $\Omega_{\rm e}$. (b) Schematics of the distribution of actin polymerization and depolymerization on the cell membrane. (c) Schematics of the distribution, strength, and direction of the active solute pumps on the cell membrane. (d) Schematics showing the shape factor of the the 2D cell.

The solvent velocity $\boldsymbol{v}_{\rm c}$ satisfies the Stokes equation with friction forces with the actin network:

$$\begin{aligned} \nabla\cdot\Sigma_{\rm m}(\boldsymbol{v}_{\rm c},p)-\eta\theta_{\rm n}(\boldsymbol{v}_{\rm c}-\boldsymbol{v}_{\rm n})=0,\ \nabla\cdot\boldsymbol{v}_{\rm c}=0,\\ \Sigma_{\rm m}(\boldsymbol{v}_{\rm c},p)=\nu\left[\nabla\boldsymbol{v}_{\rm c}+(\nabla\boldsymbol{v}_{\rm c})^T\right]-p\mathbf{I}\,, \end{aligned} \tag{III.1}$$

where $\boldsymbol{v}_{\rm n}$ is the velocity of the actin-network, ν is the dynamics viscosity of the solvent, η is the coefficient of friction between the actin network phase and the cytosol phase, and $\mathbf{I}$ is the identity matrix. The above equations are the 2D version of equation (II.12) and (II.2), the main difference being that we have viscous stresses. The friction force is present only in the $\Omega_{\rm i}$ and is set to 0 in $\Omega_{\rm e}$. The velocity of the solvent across the cell boundary satisfy $[\boldsymbol{v}_{\rm c}]=0$. The boundary condition for $\boldsymbol{v}_{\rm c}$ is

$$\boldsymbol{v}_{\rm c}-\frac{\partial\boldsymbol{X}}{\partial t}=j_{\rm water}\boldsymbol{n}\,,\qquad \text{on }\Gamma\,, \tag{III.2}$$

where $j_{\rm water}$ is the water flux across the cell membrane. The above is the 2D version of (II.10). Transmembrane water flux $j_{\rm water}$ is given by:

$$j_{\rm water}=\alpha[\psi],\qquad \psi=-RTc-\boldsymbol{n}\cdot\Sigma_{\rm m}(\boldsymbol{v}_{\rm c},p)\boldsymbol{n}, \tag{III.3}$$

where R is the ideal gas constant and T is the absolute temperature. The above expression should be compared with (II.26) and (II.18) of the 1D model. Note that, in the 1D model, a hydraulic resistance term involving the coefficient d_g had to be introduced to incorporate the effect of the external flow field. In the 2D model, this is naturally accounted for given that the external flow field is computed as part of the problem. The force balance along membrane is

$$[\Sigma_{\rm m}(\boldsymbol{v}_{\rm c},p)\boldsymbol{n}]=\sigma\boldsymbol{n}+\boldsymbol{F}_{\rm mem}\left|\frac{\partial\boldsymbol{X}}{\partial s}\right|^{-1}, \tag{III.4}$$

where σ is the pressure within the actin network defined in (III.6), and $\boldsymbol{F}_{\rm mem}$ is the membrane force defined in (III.7). The above is the 2D version of (II.16) and (II.17).

The force balance for the actin network (2D version of (II.13)) is

$$-\nabla\sigma - \eta\theta_{\rm n}(\boldsymbol{v}_{\rm n} - \boldsymbol{v}_{\rm c}) - \eta_{\rm st}\theta_{\rm n}\boldsymbol{v}_{\rm n} = 0, \tag{III.5}$$

where η_{st} is the coefficient for focal adhesion and the stress σ in actin network can be divided into a passive part $\sigma_{\rm n}$ and an active part σ_a,

$$\sigma = \sigma_{\rm n}(\theta_{\rm n}) + \sigma_{\rm a}. \tag{III.6}$$

We henceforth set $\sigma_{\rm a} = 0$. For $\sigma_{\rm n}$, we use (II.15) as in the 1D case. The membrane elastic force takes the form

$$\boldsymbol{F}_{\rm mem} = k_{\rm elas}\frac{\partial}{\partial s}\left(\left|\frac{\partial \boldsymbol{X}}{\partial s} - \frac{\partial \boldsymbol{X}_{\rm r}}{\partial s}\right|\boldsymbol{\tau}\right), \boldsymbol{\tau} = \frac{\partial \boldsymbol{X}/\partial s}{|\partial \boldsymbol{X}/\partial s|} \tag{III.7}$$

where $\boldsymbol{X}_{\rm r}$ is a target cell shape to be specified later (see (III.19)) and $k_{\rm elas}$ is the elastic modulus of the membrane. When $k_{\rm elas}$ is set to be sufficiently large, $\boldsymbol{X}$ will assume the shape traced by $\boldsymbol{X}_{\rm r}$.

The volume concentration of the actin network, $\theta_{\rm n}$, inside intracellular space, $\Omega_{\rm i}$, satisfies the conservation relation (2D version of (II.3))

$$\frac{\partial\theta_{\rm n}}{\partial t} + \nabla\cdot(\boldsymbol{v}_{\rm n}\theta_{\rm n}) = 0, \tag{III.8}$$

with boundary condition along the interior side of cell membrane (2D version of (II.11))

$$\theta_{\rm n}\Big(\frac{\partial \boldsymbol{X}}{\partial t} - \boldsymbol{v}_{\rm n}\Big)\cdot\boldsymbol{n} = j_{\rm actin}\,, \quad \text{ on } \Gamma_{\rm i}\,, \tag{III.9}$$

where $j_{\rm actin}$ describes actin polymerization and depolymerization along cell membrane. We prescribe $j_{\rm actin}$ as

$$j_{\rm actin} = k_{\rm j}(s)\left|\frac{\partial \boldsymbol{X}_0}{\partial s}\right|\left|\frac{\partial \boldsymbol{X}}{\partial s}\right|^{-1}, \tag{III.10}$$

where $k_{\rm j}(s)$ is the strength function given by

$$k_{\rm j}(s) = \begin{cases} 0\,, & \text{if } s\in(\alpha_h,\pi-\alpha_t)\cup(\pi+\alpha_t,2\pi-\alpha_h) \\ k_{\rm j}^0(s)\,, & \text{if otherwise}\end{cases}, \tag{III.11}$$

where α_h and α_t are the angular span of the regime of actin polymerization at the cell leading edge and depolymerization at the cell trailing edge, respectively (Fig. S8b), and

$$k_{\rm j}^0(s) = k_{jh}\left[e^{-s^2/h_{jl}^2} + e^{-(s-2\pi)^2/h_{jl}^2}\right] - k_{jt}e^{-(s-\pi)^2/t_{jl}^2}\,. \tag{III.12}$$

where k_{jh} (k_{jt}) scales the rate of actin polymerization (depolymerization) at the leading (trailing) edge of the cell membrane; h_{jl} and t_{jl} are the angular factors of the actin dynamics. In the model, we let $h_{jl} = \alpha_h$ and $t_{jl} = \alpha_t$. The total actin network within the cell is conserved by enforcing

$$\int_\Gamma j_{\rm actin}(s)ds = 0. \tag{III.13}$$

For solute with concentration c over the entire domain, we have (2D version of (II.21), except in the 2D case, we also consider the dynamics of the solute outside the cell):

$$\frac{\partial c}{\partial t} + \nabla \cdot (\boldsymbol{v}_{\mathrm{c}} c) = \nabla \cdot (D \nabla c) \ , \tag{III.14}$$

where D is the diffusion coefficient of the solute. The boundary condition for c is (2D version of (II.22), (II.23))

$$(\boldsymbol{v}_{\mathrm{c}} c - D \nabla c) \cdot \boldsymbol{n} = c \frac{\partial \boldsymbol{X}}{\partial t} \cdot \boldsymbol{n} + j_{\mathrm{sol}} + i_{\mathrm{sol}} \, , \quad \text{ on } \Gamma_{\mathrm{i}} \text{ or } \Gamma_{\mathrm{e}} \, , \tag{III.15}$$

where $j_{\mathrm{sol}} = k_{\mathrm{sol}}[c]$ and i_{sol} are passive and active flux of solute cross the membrane, respectively. The active flux, i_{sol}, is specified as

$$i_{\mathrm{sol}} = k_{\mathrm{p}}(s) \left| \frac{\partial \boldsymbol{X}_0}{\partial s} \right| \left| \frac{\partial \boldsymbol{X}}{\partial s} \right|^{-1} \cdot H(s), \tag{III.16}$$

where $\boldsymbol{X}_0$ is a circle with perimeter equal to the length of the cell, and

$$k_{\mathrm{p}}(s) = -k_{ph} \left[e^{-s^2/h_{pl}^2} + e^{-(s-2\pi)^2/h_{pl}^2} \right] + k_{pt} e^{-(s-\pi)^2/t_{pl}^2}, \tag{III.17}$$

$$H(s) = \begin{cases} c_{\mathrm{i}} \, , & \text{if } k_{\mathrm{p}}(s) \geq 0, \\ c_{\mathrm{e}} \, , & \text{if } k_{\mathrm{p}}(s) < 0, \end{cases} \tag{III.18}$$

where k_{ph} and k_{pt} describe the strength of the active pumps at the leading and trailing edge of the cell, respectively; h_{pl} and t_{pl} are the angular factors of the active pumps. The direction of the active solute pumping is determined by the sign of k_{p} (Eq. III.18), which effectively pumps solute into (outside of) the cell and the leading (trailing) edge (Fig. S8c).

We use a circular cell to study the impact of the physical environment on 2D cell migration (Fig. 1g in the main text). When we study the effect of cell morphology on cell migration (Fig. 4 in the main text), we fix the physical environment and vary the shape factor of the cell (Fig. S8d). In particular, we set:

$$\boldsymbol{X}_{\mathrm{r}}(s) = \begin{pmatrix} x_0 \\ y_0 \end{pmatrix} + k_{\mathrm{scale}} \begin{pmatrix} \cos s + a \cos^2 s \\ \sin s \end{pmatrix} \tag{III.19}$$

where (x_0, y_0) is the *center* of the cell, $a \geqslant 0$ measures the deviation of the cell leading edge or the trailing edge away from a circular cell and k_{scale} is s suitable scale factor. For cells with different shape factors, we maintain the same effective strength of actin polymerization or active solute pumping by prescribing these strength profiles on the material coordinate (Eqs. III.10 and III.16).

The 2D system is time dependent but steady-state can be achieved shortly after the onset of the simulation for a fixed set of parameters. We can therefore obtain a constant cell velocity for a given set of physical environment and input mechanism.

The default parameters used in the 2D model is listed in Tab. S2 unless otherwise specified. These parameters are based on the the 1D whenever applicable and are adjusted to the 2D scheme when needed. Below if a list of additional or alternative parameters. In Fig. 4(b–e), $\eta_{\mathrm{st}} = 2$ (Pa·s/μ^2m), $k_{\mathrm{sol}} = 10$ μm/s, $k_{jh} = k_{jt} = 3.4 \times 10^3$ μm/s, $k_{ph} = k_{pt} = 1.2$ μm/s. In Fig. 4(f), $k_{jh} = k_{jt} = 183.6$ μm/s. In Fig. 4(g), $k_{ph} = k_{pt} = 0.172$ μm/s. In Fig. 4(h), $k_{jh} = k_{jt} = 51$ μm/s.

TABLE S2. Parameters used in the 2D model.

Parameters	Description	Values
α (μm/Pa·s)	Water permeability	10^{-7}
C (mM)	Initial solute concentration over entire domain	340
D (μm^2/s)	Diffusion coefficient of solute	100
k_{elas} (Pa)	Elastic modulus of cell membrane	0.02
ν (Pa·s)	Dynamics viscosity of solvent	0.04
T (K)	Absolute temperature	300
ρ_{n} (mM)	Initial molar density of actin network	17
θ_0	Initial concentration of actin network	0.01
η (Pa·s/μ^2m)	Drag coefficient between two phases	0.1
η_{st} (Pa·s/μ^2m)	Coefficient of drag from focal adhesion	10^2
k_{sol} (μm/s)	Coefficient of passive solute channel	1
h_{jl}, t_{jl}, h_{pl}, t_{pl} (rad)	Angular factor of actin and pump activities	0.21π
L (μm)	Channel length and width	100
r (μm)	Radius of the cell	10

B. Numerical Algorithms

Before describing the numerical algorithm, from (II.15) and (III.8) (with $\sigma_a = 0$ and σ is used for σ_{n}), we see it is possible to solve the variable σ_{n} of actin network stress instead of θ_{n} of network concentration, by using equation (we will ignore the subscript n for the passive network stress and use σ to denote σ_{n} in the following discussions.)

$$\frac{\partial \sigma}{\partial t} + \frac{\eta}{\eta + \eta_{\text{st}}} \boldsymbol{v}_{\text{c}} \cdot \nabla \sigma = \frac{1}{\eta + \eta_{\text{st}}} \left(\frac{d\theta_{\text{n}}}{d\sigma} \right)^{-1} \nabla^2 \sigma, \tag{III.20}$$

and

$$\frac{1}{\theta_0} \theta_{\text{n}}(\sigma) = \frac{1}{RT\rho_{\text{n}}} (\sigma + \sqrt{2(RT\rho_{\text{n}})^2 + \sigma^2}), \text{ and } \frac{d\theta_{\text{n}}}{d\sigma} = \frac{\theta_0}{RT\rho_{\text{n}}} (1 + \frac{\sigma}{\sqrt{2(RT\rho_{\text{n}})^2 + \sigma^2}}). \tag{III.21}$$

Also, the velocity of actin network $\boldsymbol{v}_{\text{n}}$ can be represented by $\boldsymbol{v}_{\text{c}}$, as indicated in (III.5) and (III.6)

$$\theta_{\text{n}} \boldsymbol{v}_{\text{n}} = \frac{\eta \theta_{\text{n}} \boldsymbol{v}_{\text{c}}}{\eta + \eta_{\text{st}}} - \frac{1}{\eta + \eta_{\text{st}}} \nabla \sigma \tag{III.22}$$

And the boundary condition for θ_{n} could be converted to boundary condition for σ easily:

$$\theta_{\text{n}}(\sigma) \Big(\frac{\partial \boldsymbol{X}}{\partial t} - \frac{\eta}{\eta + \eta_{\text{st}}} \boldsymbol{v}_{\text{c}} \Big) \cdot \boldsymbol{n} + \frac{1}{\eta + \eta_{\text{st}}} \nabla \sigma \cdot \boldsymbol{n} = j_{\text{actin}}, \tag{III.23}$$

here $j_{\text{actin}}(s)$ is defined as in (III.9), and will be prescribed according to model choice.

We should note that with (III.1), (III.4), and $[\boldsymbol{v}_{\text{c}}] = 0$, the Stokes equation in (III.1) can be written in the immersed boundary formulation

$$0 = \nu \Delta \boldsymbol{v}_{\text{c}} - \eta \theta_{\text{n}} (\boldsymbol{v}_{\text{c}} - \boldsymbol{v}_{\text{n}}) - \nabla p + \boldsymbol{f}, \ \nabla \cdot \boldsymbol{v}_{\text{c}} = 0, \tag{III.24}$$

$$\boldsymbol{f}(\boldsymbol{x}, t) = \int_{\Gamma_{\text{ref}}} (\sigma \left| \frac{\partial \boldsymbol{X}}{\partial s} \right| \boldsymbol{n} + \boldsymbol{F}_{\text{mem}}(\boldsymbol{X})) \delta(\boldsymbol{x} - \boldsymbol{X}(s, t)) ds, \tag{III.25}$$

where δ is Dirac-Delta function in 2D and $\boldsymbol{F}_{\text{mem}}$ is given in (III.7).

So in the numerical algorithm, at time level t^n, we define unknown variables for solvent velocity $\boldsymbol{v}_{\text{c}}^n$, pressure p^n, solute concentration c^n, actin network stress σ^n and membrane location $\boldsymbol{X}^n$ (with discrete IB points $\boldsymbol{X}_i^n = (x_i^n, y_i^n)$, $n = 1, 2, \ldots,$ nring). It should be noted σ^n is defined in intracellular space Ω_i only and $\boldsymbol{X}^n$ is a Lagrangian variable. Those Eulerian variables p^n, σ^n, and c^n are defined at the center of each computational cell, and $\boldsymbol{v}_{\text{c}}$ is arranged according to the staggered grid setup. To facilitate the computation of discretized equations for all the unknowns, and better enforce boundary conditions for variable σ and c, we introduce auxiliary variables for both of them on either side of the elastic cell membrane (whenever it could be defined) at the places, as referred as grid crossings, where the cell membrane is intersecting the connections of neighboring computational cell centers where those two variables are defined. So we will have $\sigma_{\text{i}}^{\text{b}}$ and $c_{\text{i,e}}^{\text{b}}$ at grid crossings. Also noted is the computational cell centers next to cell membrane will be referred as *irregular* cell centers to distinguish with those cell centers (referred as *regular*) that do not have any neighbors on the other side of the cell membrane.

The outline of the overall algorithm is very similar to [15], especially the parts dealing with fluid structure interaction and solute concentration. There are modifications and new features added to account for actin network stress and are described in the following. In each time step, we first carry out the fluid-structure interaction substep, and then proceed to solve the solute concentration and network stress in two substeps sequentially.

Substep 1: Given u^n, v^n, p^n, $\theta_{\text{n}}(\sigma^n)$ and $\boldsymbol{X}^n$, use the IB method to compute u^{n+1}, v^{n+1} and p^{n+1} with a discretization of (III.24), (III.25) and (III.7). Computations of (III.25) and (III.7) is performed using $\boldsymbol{X}^n$. Once this is found, use $\boldsymbol{X}^n, c_{\text{i,e}}^{\text{b},n}$ $\sigma_{\text{i}}^{\text{b},n}$ as well as the newly found u^{n+1}, v^{n+1} to discretize (III.2) to obtain the new IB locations $\boldsymbol{X}^{n+1}$. Equation (III.2) requires solute concentration values and network stress at IB locations, which we denote by $c_{\text{i,e}}^{\text{IB},n}$ and $\sigma_{\text{i}}^{\text{IB},n}$, respectively. They are obtained by interpolating the concentration values $c_{\text{i,e}}^{\text{b},n}$ and $\sigma_{\text{i}}^{\text{b},n}$ defined at grid crossings.

Substep 2: Given our new IB point locations $\boldsymbol{X}^{n+1}$ and the fluid velocity (u^{n+1}, v^{n+1}), solve moving boundary advection diffusion problem for the concentration c^{n+1} and $c_{\text{i,e}}^{\text{b},n+1}$. At irregular cell centers discretization of equations (III.14) requires care. This is especially the case for *freshly cleared points*, which are computational cell centers that were located in Ω_{i} in the previous time step but are now in Ω_{e} or vice versa. Boundary conditions (III.15) are enforced at grid crossing with the help of the auxiliary concentration variables $c_{\text{i,e}}^{\text{b}}$. A linear system for c^{n+1} and $c_{\text{i,e}}^{\text{b},n+1}$ is obtained and solved using an iterative method.

Substep 3: Given all updated variables $\boldsymbol{X}^{n+1}$, the fluid velocity (u^{n+1}, v^{n+1}), solute c^{n+1} and $c_{\text{i,e}}^{\text{b},n+1}$, solve moving boundary nonlinear advection diffusion problem for the network stress σ^{n+1} and $\sigma_{\text{i}}^{\text{b},n+1}$. At irregular cell centers and freshly cleared points, discretization of equations (III.20) requires same care as in substep 2. Boundary conditions (III.23) are enforced at grid crossing with the help of the auxiliary variable $\sigma_{\text{i}}^{\text{b}}$. A linear system for σ^{n+1} and $\sigma_{\text{i}}^{\text{b},n+1}$, which is smaller than the one obtained in substep 2, is obtained and solved using an iterative method.

We note in both substep 2 and 3, to enforce boundary conditions, $\partial \boldsymbol{X}/\partial t$ could be replaced by $\boldsymbol{v}_{\text{c}}$ in (III.2) to increase computational stability. Now we discuss each computational substep in detail.

1. Fluid structure interaction substep

As we mentioned before, the pressure p is defined at cell centers and the velocity field $\boldsymbol{v}_{\mathrm{c}}$ is defined at the horizontal (u) and vertical (v) cell faces. Define the following differencing operators for any grid function w, where $w^n_{\alpha,\beta}$ denotes the value of w at $(x,y)=(\alpha h,\beta h)$ at time $t=n\triangle t$:

$$\begin{aligned}\mathcal{D}_x^{\pm} w_{\alpha,\beta} &= \pm\frac{w_{\alpha\pm1,\beta}-w_{\alpha,\beta}}{h}, \quad \mathcal{D}_y^{\pm} w_{\alpha,\beta} = \pm\frac{w_{\alpha,\beta\pm1}-w_{\alpha,\beta}}{h},\\ \mathcal{L} w_{\alpha,\beta} &= \mathcal{D}_x^{+}\mathcal{D}_x^{-} w_{\alpha,\beta} + \mathcal{D}_y^{+}\mathcal{D}_y^{-} w_{\alpha,\beta}\\ &= \frac{w_{\alpha+1,\beta}+w_{\alpha,\beta+1}+w_{\alpha-1,\beta}+w_{\alpha,\beta-1}-4w_{\alpha,\beta}}{h^2},\end{aligned} \tag{III.26}$$

Let $\boldsymbol{v}_{\mathrm{c}}=(u,v)$, $\boldsymbol{v}_{\mathrm{n}}=(\tilde{u},\tilde{v})$, and $\boldsymbol{f}=(f,g)$, equation (III.24) is then

$$\begin{aligned}\mathcal{D}_x^{-} p^{n+1}_{i+\frac12,j+\frac12} &= \nu\mathcal{L}u^{n+1}_{i,j+\frac12} + \eta\theta_{\mathrm{n},i,j+\frac12}(u^n_{i,j+\frac12}-\tilde{u}^n_{i,j+\frac12}) + f^n_{i,j+\frac12},\\ \mathcal{D}_y^{-} p^{n+1}_{i+\frac12,j+\frac12} &= \nu\mathcal{L}v^{n+1}_{i+\frac12,j} + \eta\theta_{\mathrm{n},i,j+\frac12}(v^n_{i+\frac12,j}-\tilde{v}^n_{i+\frac12,j}) + g^n_{i+\frac12,j},\\ 0 &= \mathcal{D}_x^{-} u^{n+1}_{i+1,j+\frac12} + \mathcal{D}_y^{-} v^{n+1}_{i+\frac12,j+1}.\end{aligned} \tag{III.27}$$

As we assume periodic boundary condition for $\boldsymbol{v}_{\mathrm{c}}$ and p on the left and right edge of the computational domain, and homogeneous Dirichlet boundary condition for $\boldsymbol{u}$ on the top and bottom edges, we can solve (u,v) and p from linear system (III.27) by using FFT along x direction, which will result in block diagonal linear system to solve at each x_i, and can be solved efficiently using a direct solver.

We turn to the determination of the body forces $\boldsymbol{f}=(f,g)$. Let $\boldsymbol{F}_{\mathrm{mem}}=(F_x,F_y)$, $\boldsymbol{n}=(n_x,n_y)$ and the IB point positions $\boldsymbol{X}=(X,Y)$. For a quantity W defined on the immersed boundary grid parametrized by s, we let W_k denote the value of W at point $s=s_k=k\triangle s$, where $\triangle s$ is the grid spacing in s. Equation (III.25) for $\boldsymbol{f}=(f,g)$ are discretized as follows

$$\begin{aligned}f^n_{i,j+\frac12} &= \sum_{k=1}^{N_{\mathrm{ring}}}(\sigma^n n^n_x\left|\frac{\partial \boldsymbol{X}^n}{\partial s}\right| + F^n_{x,k})\delta_h(x_i-X^n_k)\delta_h(y_{j+\frac12}-Y^n_k)\triangle s\\ g^n_{i+\frac12,j} &= \sum_{k=1}^{N_{\mathrm{ring}}}(\sigma^n n^n_y\left|\frac{\partial \boldsymbol{X}^n}{\partial s}\right| + F^n_{y,k})\delta_h(x_{i+\frac12}-X^n_k)\delta_h(y_j-Y^n_k)\triangle s\end{aligned} \tag{III.28}$$

where $\delta_h(r)$ is a regularized discrete delta function. In this paper, we use the one in [15]. To compute the membrane force $\boldsymbol{F}_{\mathrm{mem}}$ let us first introduce the following differencing operators acting on functions W defined on the IB grid:

$$\mathcal{D}_s^{\pm} W_k = \pm\frac{W_{k\pm1}-W_k}{\triangle s},\ \mathcal{L}_s W_k = \mathcal{D}_s^{+}\mathcal{D}_s^{-} W_k. \tag{III.29}$$

Using these operators, we discretize (III.25) as follows:

$$\boldsymbol{F}^n_{\mathrm{mem},k} = k_{\mathrm{elas}}\mathcal{D}_s^{+}\left(\left(1-\ell\left|\mathcal{D}_s^{-}\boldsymbol{X}^n_k\right|^{-1}\right)\mathcal{D}_s^{-}\boldsymbol{X}^n_k\right) - k_{\mathrm{bend}}\mathcal{L}_s\mathcal{L}_s\boldsymbol{X}^n_k, \tag{III.30}$$

where the differencing operators above act component-wise.

2. Semi-implicit update of IB locations

We turn to the update of the IB point locations. In the discretization of equation (III.2), we employ the following scheme:

$$\begin{aligned}
\mathcal{D}_t^- \boldsymbol{X}_k^{n+1} &= \boldsymbol{U}_k^{n+1} - j_{\text{water}}^n,\ j_{\text{water}}^n = -\alpha \left(\left[c_k^{\text{IB},n} \right] + \sigma_k^{\text{IB},n} + \widehat{\boldsymbol{F}}_{\text{mem},k}^{n+1} \cdot \boldsymbol{n}^n \right),\ \boldsymbol{U}_k = (U_k, V_k), \\
\widehat{\boldsymbol{F}}_{\text{mem},k}^{n+1} &= \boldsymbol{F}_{\text{mem},k}^{n+1} \frac{1}{2} \left(\left| \mathcal{D}_s^+ \boldsymbol{X}^n \right|^{-1} + \left| \mathcal{D}_s^- \boldsymbol{X}^n \right|^{-1} \right), \\
U_k^n &= \sum_{i,j} u_{i,j+\frac{1}{2}}^n \delta_h(x_i - X_k^n) \delta_h(y_{j+\frac{1}{2}} - Y_k^n) h^2, \\
V_k^n &= \sum_{i,j} v_{i+\frac{1}{2},j}^n \delta_h(x_{i+\frac{1}{2}} - X_k^n) \delta_h(y_j - Y_k^n) h^2,
\end{aligned} \tag{III.31}$$

where $\boldsymbol{F}_{\text{mem,k}}^{n+1}$ is specified as in (III.30), and

$$\mathcal{D}_t^- (\cdot)^n = \frac{(\cdot)^n - (\cdot)^{n-1}}{\triangle t} \tag{III.32}$$

The values $c_{\text{i,e},k}^{\text{IB},n}$ are the intracellular and extracellular concentrations at the IB point k at time $n\triangle t$, and is evaluated by interpolating the membrane concentration values at grid crossings $c_{\text{i,e}}^{\text{b},n}$. Similar is done for $\sigma_k^{\text{IB},n}$. The jump $\left[c_k^{\text{IB},n} \right]$ is equal to $c_{\text{i},k}^{\text{IB},n} - c_{\text{e},k}^{\text{IB},n}$. In the right hand side of the first equation, all terms except for $\boldsymbol{F}_{\text{mem,k}}$ are known quantities. This is thus a nonlinear equation for $\boldsymbol{X}^{n+1}$, which is solved using a Newton iteration. We have found that the implicit treatment of $\boldsymbol{F}_{\text{mem,k}}$ lead to better stability properties.

3. Chemical concentration substep

We will describe the solute concentration substep in detail as the method presented here will be used for computing network stress again.

The regular cell centers have no neighboring grid cell centers on the other side of the membrane Γ_{n+1}, the immersed boundary defined by the IB point locations $\boldsymbol{X}^{n+1}$.

At any regular Cartesian cell center, we use a standard implicit Euler discretization of the (III.14):

$$\mathcal{D}_t^- c_{i+\frac{1}{2},j+\frac{1}{2}}^{n+1} + \mathcal{D}_x^- \left(u_{i+1,j+\frac{1}{2}}^{n+1} \mathcal{A}_x^+ c_{i+\frac{1}{2}j+\frac{1}{2}}^{n+1} \right) + \mathcal{D}_y^- \left(v_{i+\frac{1}{2},j+1}^{n+1} \mathcal{A}_y^+ c_{i+\frac{1}{2}j+\frac{1}{2}}^{n+1} \right) = D\mathcal{L} c_{i+\frac{1}{2},j+\frac{1}{2}}^{n+1}, \tag{III.33}$$

in which, for any quantity w on the Cartesian grid,

$$\mathcal{A}_x^+ w_{\alpha,\beta} = \frac{1}{2} \left(w_{\alpha+1,\beta} + w_{\alpha,\beta} \right),\ \mathcal{A}_y^+ w_{\alpha,\beta} = \frac{1}{2} \left(w_{\alpha,\beta+1} + w_{\alpha,\beta} \right), \tag{III.34}$$

where α, β are integer or half integer. Note here that the velocity field (u^{n+1}, v^{n+1}) have been determined at the fluid structure interaction substep.

For solutes at irregular cell centers, we use (III.48) but with the following modifications. Suppose we try to update the solute c_A^{n+1} defined at cell center A (contained in Ω_{i}) in left panel of the Figure S9 using (III.48). The difference operators require solute concentration variables at p_1 and p_3. We obtain an expression for the concentration at these two points (called *ghost cells*) with an

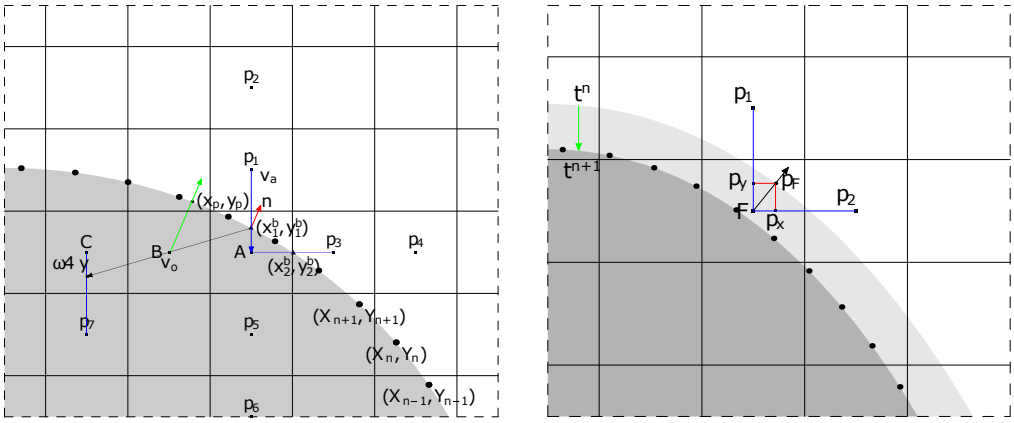

FIG. S9. Treatment of freshly cleared grid

extrapolation procedure using concentration variables at the cell centers and grid crossings in $\Omega_{\rm i}$ (where point A is located).

The extrapolation scheme for ghost cell solutes is adopted from [16]. At point p_1, in left panel of Fig. S9, we use

$$c_{p_1} = \frac{2(1-\omega)}{2+\omega} c_{p_6} - \frac{3(1-\omega)}{1+\omega} c_{p_5} + \frac{6}{(1+\omega)(2+\omega)} c_{\rm i}^{\rm b}, \tag{III.35}$$

where ω is the ratio of distance from the grid crossing $(x_1^{\rm b}, y_1^{\rm b})$ to A and distance from p_1 to A (grid spacing in the y direction), c_{p_6} and c_{p_5} are solutes at p_6 and p_5 respectively, and $c_{\rm i}^{\rm b}$ is the auxiliary intracellular solute concentration defined at grid crossing $(x_1^{\rm b}, y_1^{\rm b})$. A similar procedure is performed in the x direction to obtain an extrapolation formula at point p_3.

Equation (III.35) uses two grid point locations p_5 and p_6, and in exceptional cases depending on the geometry of Γ relative to the Cartesian grid, two such grid points may not be available. When only one such point is available, we use the formula:

$$c_{p_1} = \frac{-(1-\omega)}{1+\omega} c_{p_5} + \frac{2}{(1+\omega)} c_{\rm i}^{\rm b}. \tag{III.36}$$

In the extreme case when no such grid locations are available, we set $c_{p_1} = c_{\rm i}^{\rm b}$. The use of these lower order extrapolation procedures (as opposed to (III.35)) will in general lead to order 1 consistency errors at these grid points. However, the points at which such errors are committed remains a small fraction of cell centers (the proportion should become smaller with finer grid spacing), and thus does not affect the order of convergence, as is documented in [16] and demonstrated below.

These extrapolation formulae are substituted into the corresponding terms in (III.48) to produce the spatial stencil at the irregular cell centers. The stencil at the irregular stencils, therefore, depend not only on concentration values at cell centers but also at grid crossings $c_{\rm i}^{\rm b}$ or $c_{\rm e}^{\rm b}$.

4. Time discretization at freshly cleared cell

At a freshly cleared cell we must modify the time discretization. Such modifications are discussed in [17, 18]. Here, we propose new procedure which is simple to implement with good stability properties.

Consider the point F in the right panel of Figure S9. It is a freshly cleared point that was in $\Omega_{\rm i}$ at time $t = n\triangle t$ but is in $\Omega_{\rm e}$ at $t = (n+1)\triangle t$. In evaluating the time differencing term in

(III.48) at this point, c_F^n has to be available. Since point F was not in Ω_e at time level n, c_F^n is not available. A standard way to obtain this value is to extrapolate the $t = n\triangle t$ level solutes at neighbor cell centers, at p_1 and p_2, say, on the intracellular side, to F . This extrapolation could lead to large numerical errors especially in extreme geometric situations. Here we propose a new scheme for the discretization of the time derivative.

First we find the point $p_F = (x_F^*, y_F^*) \in \Gamma_n$ that is closest to the point $F = (x_F, y_F)$. The solute concentration at point p_F at time $t = n\triangle t$ (on the extracellular side, which we call c^n_{e,p_F}) may be obtained by interpolating the solute concentration values at grid crossings $c_\mathrm{e}^{\mathrm{b},n}$ at time $t = n\triangle t$. A (seemingly) reasonable approximation to the partial time derivative at point F would be:

$$\frac{c_F^{n+1} - c^n_{\mathrm{e},p_F}}{\triangle t}. \tag{III.37}$$

The above expression, however, will not be a consistent discretization because this differencing corresponds to an "advective" derivative. The velocity of this advection is given by:

$$(\widetilde{u}_F, \widetilde{v}_F) = \left(\frac{x_F - x_F^*}{\triangle t}, \frac{y_F - y_F^*}{\triangle t} \right). \tag{III.38}$$

Therefore, (III.37) must be corrected to remove the advective component resulting from the above velocity. The following is thus a consistent discretization of the time derivative of concentration c_F at point F:

$$\left.\frac{\partial c_F}{\partial t}\right|_{t=n\triangle t} \approx \frac{c_F^{n+1} - c^n_{\mathrm{e},p_F}}{\triangle t} - \widetilde{u}_F \mathcal{D}^0_x c_F^{n+1} - \widetilde{v}_F \mathcal{D}^0_y c_F^{n+1}. \tag{III.39}$$

where

$$\mathcal{D}^0_{x,y} w = \frac{1}{2}\left(\mathcal{D}^+_{x,y} w + \mathcal{D}^-_{x,y} w \right). \tag{III.40}$$

At freshly cleared points, expression (III.39) is used in place of the $\mathcal{D}_t^- c$ term in (III.48). The above spatial differencing in many cases involves ghost cell locations. In such cases, extrapolation formulae discussed in previous subsection are used.

5. Enforcing solute boundary condition with auxiliary variables

The solute boundary conditions (III.15) are enforced along the membrane $\Gamma_{\mathrm{i,e}}$, with the help of the auxiliary solutes defined at grid crossings on both sides of the interface. We first rewrite boundary condition (III.15) using (III.2) and (III.16):

$$j_\mathrm{w} c - D\nabla c \cdot \boldsymbol{n} = k_\mathrm{sol}[c] + \widehat{k}_\mathrm{p} H(s, c_\mathrm{i}, c_\mathrm{e}). \tag{III.41}$$

Let us consider grid crossing $(x_1^\mathrm{b}, y_1^\mathrm{b})$ as in the left panel of Figure S9. The above boundary condition is satisfied on both sides of the membrane. We consider the Ω_i side of the membrane. Our discretization of (III.41) is:

$$j_\mathrm{w}^n c_\mathrm{i}^n - D\mathcal{N}(c_\mathrm{i}^{\mathrm{b},n+1}, c^{n+1}) = k_\mathrm{sol}[c^{\mathrm{b},n+1}] + \widehat{k}_\mathrm{p} H(s, c_\mathrm{i}^n, c_\mathrm{e}^n). \tag{III.42}$$

The diffusive flux term and the passive membrane flux term are treated implicitly at time $t = (n+1)\triangle t$. This implicit treatment of the boundary condition is the key to stable computations. Our computational experience indicates that an explicit treatment of these terms leads to persistent

spurious oscillations of the solute concentrations near the interfacial boundary. The other terms are evaluated at explicitly, but we point out that these values are not available at the grid crossings; the above equations are defined on the grid crossings at $t = (n+1)\triangle t$ but grid crossings change with every time step. We compute these terms in the following fashion. We take j^n_{water} and c^n defined at IB points (see equation (III.31)) and assign these values to the corresponding IB points at time $t = (n+1)\triangle t$. Then, we interpolate these values to the grid crossing locations.

We now discuss the discretization of the normal derivative (the $\mathcal{N}$ term in (III.42)). Our procedure follows [16]. Taking intracellular side of the grid crossing at (x^b_1, y^b_1) in the left panel of Figure S9, the treatment is illustrated as follows.

The unit normal direction $\boldsymbol{n}$ along Γ can be decomposed into two directions: along grid line $\boldsymbol{v}_a$ (from point p_1 to A); and off grid line $\boldsymbol{v}_o$ (from boundary point (x^b_1, y^b_1) through grid point B and stop on grid line between C and p_7). We thus have $\boldsymbol{n} = a_o\boldsymbol{v}_o + a_a\boldsymbol{v}_a$. With these two directions, the normal derivative $\nabla c^{\text{b}}_{\text{i}} \cdot \boldsymbol{n}$ can be decomposed as a linear combination of directional derivatives along the $\boldsymbol{v}_o$ and $\boldsymbol{v}_a$ directions:

$$\begin{aligned}\nabla c^{\text{b}}_{\text{i}} \cdot \boldsymbol{n} &= a_o \nabla c^{\text{b}}_{\text{i}} \cdot \boldsymbol{v}_o + a_a \nabla c^{\text{b}}_{\text{i}} \cdot \boldsymbol{v}_a \\ &= a_o ||\boldsymbol{v}_o|| \frac{\partial c^{\text{b}}_{\text{i}}}{\partial(\boldsymbol{v}_o/||\boldsymbol{v}_o||)} + a_a ||\boldsymbol{v}_a|| \frac{\partial c^{\text{b}}_{\text{i}}}{\partial(\boldsymbol{v}_a/||\boldsymbol{v}_a||)}.\end{aligned} \tag{III.43}$$

So along $\boldsymbol{v}_o$ and $\boldsymbol{v}_a$, we need to approximate the partial derivatives, using solutes at cell centers and the auxiliary variables at grid crossings. If a first order approximation is used, we will have

$$\nabla c^{\text{b}}_{\text{i}} \cdot \boldsymbol{n} \approx a_o(c_B - c^{\text{b}}_{\text{i}}) + a_a(c_{p_5} - c^{\text{b}}_{\text{i}}), \tag{III.44}$$

where c_B is the solute at point B, and c^{b}_{i} is auxiliary solute at the grid crossing on intracellular side. The direction vectors are given by

$$\boldsymbol{v}_o = (x_B - x^b_1, y_B - y^b_1), \ \boldsymbol{v}_a = (x_{p_5} - x^b_1, y_{p_5} - y^b_1). \tag{III.45}$$

In choosing the cell centers used for this process, we avoid using cell centers that are directly adjacent to the grid crossing. Otherwise, $\boldsymbol{v}_o$ or $\boldsymbol{v}_a$ can be arbitrarily small in length, and the coefficient a_o and a_a can become arbitrarily large thus leading to possible numerical instabilities.

We use higher order approximations if more cell centers are available. For example if instead of just using point B for the off grid line direction, we may use point B, C, and p_7

$$\frac{\partial c^{\text{b}}_{\text{i}}}{\partial(\boldsymbol{v}_o/||\boldsymbol{v}_o||)} \approx -\frac{3}{2||\boldsymbol{v}_o||}c^{\text{b}}_{\text{i}} + \frac{2}{||\boldsymbol{v}_o||}c_B - \frac{1}{2||\boldsymbol{v}_o||}[(1-\omega)c_C + \omega c_{p_7}], \tag{III.46}$$

and if we use the grid crossing, point p_5 and p_6, we have

$$\frac{\partial c^{\text{b}}_{\text{i}}}{\partial(\boldsymbol{v}_a/||\boldsymbol{v}_a||)} \approx -\frac{1+\omega}{(2+\omega)\triangle y}c_{p_6} + \frac{2+\omega}{(1+\omega)\triangle y}c_{p_5} - \frac{3+2\omega}{(1+\omega)(2+\omega)\triangle y}c^{\text{b}}_{\text{i}}. \tag{III.47}$$

The ω here in (III.47) and (III.46) is the same as in (III.35).

6. Network stress substep

At any regular Cartesian cell center in Ω_{i}, we use a standard implicit Euler discretization of the (III.20):

$$\mathcal{D}^-_t \sigma^{n+1}_{i+\frac{1}{2},j+\frac{1}{2}} + \frac{\eta}{\eta+\eta_{\text{st}}}\left\{\mathcal{D}^-_x\left(u^{n+1}_{i+1,j+\frac{1}{2}}\mathcal{A}^+_x\sigma^{n+1}_{i+\frac{1}{2}j+\frac{1}{2}}\right) + \mathcal{D}^-_y\left(v^{n+1}_{i+\frac{1}{2},j+1}\mathcal{A}^+_y\sigma^{n+1}_{i+\frac{1}{2}j+\frac{1}{2}}\right)\right\} = \tilde{D}\mathcal{L}\sigma^{n+1}_{i+\frac{1}{2},j+\frac{1}{2}}, \tag{III.48}$$

where all difference operators are defined as in previous subsections, velocity field (u^{n+1}, v^{n+1}) have been determined at the fluid structure interaction substep, and the nonlinear diffusion coefficient $\tilde{D}$ is

$$\tilde{D} = \frac{1}{\eta + \eta_{\rm st}} \frac{d\theta_{\rm n}(\sigma^n_{i+\frac{1}{2}j+\frac{1}{2}})^{-1}}{d\sigma}. \tag{III.49}$$

We note all special cares needed for handling irregular cell centers, freshly cleared points and enforcing boundary conditions are discussed in previous sections for solute concentration c, especially for c in $\Omega_{\rm i}$, and here we will not put in more details. But we point out that when enforcing boundary conditions using (III.2) in (III.23), $[c]$ should use the solutes from substep 2 which are just updated.

C. Mechanical Energy Identities

Similar to the 1D model, the 2D model satisfies energy identities,

$$\frac{d}{dt}(G_s + E_{\rm n} + E_{\rm mem}) = -(I_{\rm f} + I_{\rm n} + I_{\rm m}) + J_{\rm m}, \tag{III.50}$$

where

$$G_{\rm s} = \int_{\Omega_{\rm i}\cup\Omega_{\rm e}} \omega d\boldsymbol{x},\ \omega = RT(c\ln c - c),\ E_n = \int_{\Omega_i} e_n d\boldsymbol{x} \tag{III.51}$$

$$E_{\rm mem} = \int_{\Gamma_{\rm ref}} \left(k_{\rm elas}\left(\left|\frac{\partial \boldsymbol{X}}{\partial s}\right|\right)^2 + k_{\rm bend}\left|\frac{\partial^2 \boldsymbol{X}}{\partial s^2}\right|^2 \right) ds, \tag{III.52}$$

$$I_{\rm f} = \int_{\Omega_{\rm i}\cup\Omega_{\rm e}} \left(\nu\left|\nabla \boldsymbol{v}_{\rm c} + (\nabla \boldsymbol{v}_{\rm c})^T\right|^2 + \frac{D}{RT} c\left|\nabla\mu\right|^2 \right) d\boldsymbol{x},\ \mu = RT\ln c, \tag{III.53}$$

$$I_{\rm n} = \int_{\Omega_i} \left(\eta\theta_{\rm n}|\boldsymbol{v}_{\rm c} - \boldsymbol{v}_{\rm n}|^2 + \eta_{\rm st}\theta_{\rm n}|\boldsymbol{v}_{\rm n}|^2\right) d\boldsymbol{x},\ I_m = \int_\Gamma \left(k_{\rm sol}[c][\mu] + \alpha[\psi]^2\right) dm_\Gamma \tag{III.54}$$

$$J_{\rm m} = \int_\Gamma \left(\frac{de_n}{d\theta_{\rm n}} j_{\rm actin} - [\mu] i_{\rm sol} \right) dm_\Gamma,\ dm_\Gamma = \left|\frac{\partial \boldsymbol{X}}{\partial s}\right| ds, \tag{III.55}$$

where the network energy density e_n is determined by

$$\theta_{\rm n}\frac{de_n}{d\theta_{\rm n}} - e_n = \sigma_{\rm n}(\theta_{\rm n}). \tag{III.56}$$

Under steady-state, $J_{\rm m} = I_{\rm f} + I_{\rm n} + I_{\rm m}$. The mechanical energy consumption is calculated from $J_{\rm m}$ when steady-state is reached. Each power consumption term is in the dimensional of Watt per unit length. We obtain the power consumption in Watt by multiplying the terms in Eq. (III.50) by the effective height of the cell, which is approximated as 1 μm.

---

[1] B. L. Bangasser, G. A. Shamsan, C. E. Chan, K. N. Opoku, E. Tüzel, B. W. Schlichtmann, J. A. Kasim, B. J. Fuller, B. R. McCullough, S. S. Rosenfeld, and D. J. Odde, Nat. Commun. **8**, 15313 (2017).

[2] S. Walcott and S. X. Sun, Proc. Natl. Acad. Sci. **107**, 7757 (2010).

[3] D.-H. Kim and D. Wirtz, FASEB J. **27**, 1351 (2013).

[4] E. A. Cavalcanti-Adam, T. Volberg, A. Micoulet, H. Kessler, B. Geiger, and J. P. Spatz, Biophys. J. **92**, 2964 (2007).
[5] F. Horkay and G. B. McKenna, in *Physical properties of polymers handbook* (Springer, 2007) pp. 497–523.
[6] H. Jiang and S. X. Sun, Biophys. J. **105**, 609 (2013).
[7] M. Dembo and F. Harlow, Biophys. J. **50**, 109 (1986).
[8] K. M. Stroka, H. Jiang, S.-H. Chen, Z. Tong, D. Wirtz, S. X. Sun, and K. Konstantopoulos, Cell **157**, 611 (2014).
[9] M. L. Gardel, B. Sabass, L. Ji, G. Danuser, U. S. Schwarz, and C. M. Waterman, J. Cell. Biol. **183**, 999 (2008).
[10] R. L. Satcher and C. F. Dewey, Biophys. J. **71**, 109 (1996).
[11] M. J. Footer, J. W. J. Kerssemakers, J. A. Theriot, and M. Dogterom, Proc. Natl. Acad. Sci. USA **104**, 2181 (2007).
[12] G. M. Cooper, R. E. Hausman, and R. E. Hausman, *The Cell: A Molecular Approach*, Vol. 10 (ASM press Washington, DC, 2000).
[13] K. C. Holmes, D. Popp, W. Gebhard, and W. Kabsch, Nature **347**, 44 (1990).
[14] H. Wang and G. Oster, Nature **396**, 279 (1998).
[15] L. Yao and Y. Mori, J. Comput. Phys. **350**, 728 (2017).
[16] P. Macklin and J. S. Lowengrub, J. Sci. Comput. **35**, 266 (2008).
[17] P. McCorquodale, P. Colella, and H. Johansen, J. Comput. Phys. **173**, 620 (2001).
[18] J. Yang and E. Balaras, J. Comput. Phys. **215**, 12 (2006).